Haggerty, J.A., Premoli Silva, I., Rack, F., and McNutt, M.K. (Eds.), 1995
Proceedings of the Ocean Drilling Program, Scientific Results, Vol. 144

47. A MODEL FOR DEPOSITIONAL SEQUENCES AND SYSTEMS TRACTS ON SMALL, MID-OCEAN CARBONATE PLATFORMS: EXAMPLES FROM WODEJEBATO (SITES 873–877) AND LIMALOK (SITE 871) GUYOTS[1]

Annie Arnaud Vanneau,[2] Douglas D. Bergersen,[3] Gilbert F. Camoin,[4] Philippe Ebren,[4] Janet A. Haggerty,[5] James G. Ogg,[6] Isabella Premoli Silva,[7] and Peter R. Vail[8]

ABSTRACT

Classic sequence stratigraphy concepts were applied to small, mid-ocean carbonate platforms (maximum diameter of approximately 40 km) in the Pacific Ocean to explain the lithologic, stratigraphic, faunal, and stratal pattern changes observed in core and seismic data. Changes in faunal assemblages define major sequence units, whereas emergence surfaces, marked by subaerial erosion, cemented limestones, and sometimes karstification represent sequence boundaries. Lowstand systems tracts are not identifiable along the perimeter of the summit plateaus but occur as turbidites in the adjacent archipelagic apron deposits. Transgressive and highstand systems tracts generally appear as aggrading units in the seismic data; an exception exists with the lowermost transgressive systems tract, where retrogradational reflectors onlap an irregular reflector interpreted as seismic basement. Increased abundances of planktonic species mark maximum flooding surfaces. The absence of transitional sediments between the last platform carbonates and the first pelagic sediments leads us to postulate that the demise of these carbonate platforms relates to a rapid fall in sea level (causing a cessation in carbonate production), followed by a rapid rise that outstripped the rate of carbonate production.

INTRODUCTION

Seismic and sequence stratigraphy concepts (e.g., Vail et al., 1977; Van Wagoner et al., 1988; Wilgus et al., 1988; Walker, 1990) have undergone considerable refinement over the past decade. These ideas, initially developed from seismic data collected over siliciclastic systems along passive margins and subsequently extended to mixed carbonate/siliciclastic and pure carbonate environments (Sarg, 1988; Arnaud Vanneau et al., 1990; Jacquin et al., 1991; Handford and Loucks, 1993), have improved our understanding of how depositional systems (e.g., environments and stratal geometry variations) respond to relative changes in sea level. Ideally, sequence stratigraphy interpretations integrate high-quality core samples, precise paleontological data, and well-log data with seismic data to differentiate systems tracts and the influence of eustatic sea-level changes from such factors as plate subsidence and sediment compaction. The generally poor recovery during Leg 144 drilling precludes an independent estimate of sea-level change. As such, sequence boundaries and systems tracts identified in the data are compared with postulated sea-level changes shown in the eustatic curve of Haq et al. (1987).

Of the five guyots drilled during Leg 144, only two of the edifices have core samples, well-log data, and seismic data of sufficient quality to attempt a sequence stratigraphy interpretation. These two guyots, Wodejebato and Limalok in the Marshall Islands, are the submerged members of atoll/guyot pairs. Wodejebato Guyot (12.0°N, 164.9°E) lies in the northern part of Ralik Chain, 74 km northwest of Pikinni Atoll. Limalok Guyot (5.6°N, 172.3°E) lies in the southern portion of the Ratak Chain, 54 km from Mili Atoll. (See site map preceding title page.) Descriptions of the physiographic and stratigraphic variations observed across these platforms can be found in Bergersen (1993), Bergersen (this volume), Camoin et al. (this volume), and Wyatt et al. (this volume). By integrating the information from seismic profiles, well logs, and sediment and paleontology studies with the sequence stratigraphy concept, we propose a model for these small mid-ocean tropical carbonate platforms.

SEQUENCE STRATIGRAPHY OF THE GUYOTS

Guyots are very small islands (<50 km long) with a flat summit plateau and steep upper slopes (>20°). According to the morphology, this type of platform can be referred to as a rimmed shelf with a bypass margin (Read, 1985). They are not true reefal islands; corals are not always present and abundant, in which case red algae and mollusks are frequent.

Depositional sequences, according to the sequence stratigraphy model, consist of lowstand (LST), transgressive (TST), and highstand (HST) systems tracts. On the small mid-ocean carbonate platforms examined in this study, the TST and HST systems tracts were the predominant depositional style.

Carbonate platform sequence boundaries are usually quite detectable on these guyots. The summit of the volcano is practically flat; therefore, when sea level falls, the platform emerges and is affected by subaerial exposure and subsequent erosion. Subaerial exposure can result in dissolution, cementation, and karstification of the carbonate sediments. If well-cemented sediments underlie the sequence boundary, acoustic impedance contrasts with the overlying sediments and may produce a reflector in the seismic data as well as a pronounced shift in resistivity in the well-log data. Diagenetic anomalies linked to subaerial exposure (e.g., karstic dissolutions and cementation, meteoric-vadose dissolution and cementation, and fresh-water cementation) can be identified by diagenetic and isotopic analyses (e.g., Durlet et al., 1992; Vollbrecht and Meischner, 1993; Arnaud Vanneau and Carrio-Schaffauser, 1994). Dolomitization located just below the sequence boundary is also evidence for subaerial exposure.

[1] Haggerty, J.A., Premoli Silva, I., Rack, F., and McNutt, M.K. (Eds.), 1995. *Proc. ODP, Sci. Results,* 144: College Station, TX (Ocean Drilling Program).
[2] URA 69, Institut Dolomieu, Laboratoire de Géodynamique des Chaînes Alpines, 15 rue Maurice Gignoux, 38031 Grenoble cedex, France.
[3] University of Sydney, Department of Geology, N.S.W. 2006, Australia.
[4] URA 1208, Université de Provence, Centre de Sédimentologie, 3 Place Victor Hugo, 13331 Marseille cedex 3, France.
[5] University of Tulsa, Department of Geosciences, 600 South College Avenue, Tulsa, OK 74104, U.S.A.
[6] Purdue University, Department of Earth and Atmospheric Sciences, West Lafayette, IN 47907, U.S.A.
[7] Università di Milano, Dipartimento di Scienze della Terra, via Mangiagalli 34, 20133 Milano, Italy.
[8] Rice University, Department of Geology and Geophysics, Houston, TX 77251, U.S.A.

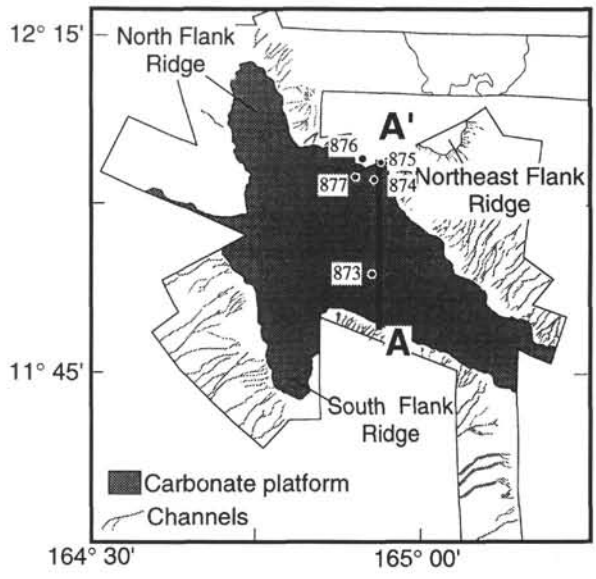

Figure 1. Areal distribution of the carbonate platform of Wodejebato Guyot (after Camoin et al., this volume). A–A′: location of the seismic profile and sites.

Truncated reflectors and toplap surfaces in seismic data also mark erosional surfaces (Sarg, 1988).

Lowstand systems tracts are not always present, except on the narrow edge of the guyot when the volcano was flooded for the first time and just before the demise of the carbonate platform when the last carbonate sediments deposited on the edge of the platform can be considered as an example of a forced regression. During this time, no deposition occurred across the summit plateau; if the time duration of the sea-level lowstand is sufficient, the sequence boundary may correspond to a significant sedimentologic and paleontologic gap that cannot be dated by the youngest fauna found in the overlying sediments. The platform margin can be eroded. Sediments can slide on the slope and resediment at the toe of the slope and into the basin. Lowstand carbonate turbidites may contain skeletal grains and clasts derived from older sediments associated to penecontemporaneous sediments.

Transgressive systems tracts are of two types. The first type corresponds to the first TST systems tract associated with the first flooding of the volcano. The first carbonate factory must tolerate clay inputs, an environment that seems favorable to the development of red algae and rhodoliths. During the following TST systems tracts, clay inputs are reduced or missing, and sediments are mostly carbonates. The morphology is also different. The first TST is well developed above an irregular surface, and onlaps are well expressed. The following TST systems tracts are disposed on a flat plateau, and onlaps are not always visible. In every case, the transgressive sediments at the bottom of TST systems tracts are a mixture of reworked and broken fossils, reworked clasts from the underlying sequence, and new species.

During a TST systems tract, the rate of sea-level rise increases up to the maximum flooding stage, and the carbonate factory backsteps toward the central basement high. In the early stages, the rate of carbonate production exceeds the rate of sea-level rise, and the carbonate factory grows upward to sea level. Such carbonate successions are called "catch-up series" (James and Macintyre, 1985). When ecological factors change to the point that bioclasts of the carbonate factory become smaller (foraminifers) or thinner (metazoans), the rate of sea-level rise exceeds the rate of carbonate production. Such series are known as "give-up series." Planktonic foraminifers and calcareous nannofossils progressively invade the platform as it is flooded; an increased abundance of planktonic species is a key marker for the maximum flooding surface.

During the HST systems tract, the rate of sea-level rise diminishes to the point of becoming stable. If the carbonate factory is still able to produce sediments, the platform begins to aggrade. During the early HST systems tract, the production rate matches the rate of relative sea-level rise and the carbonate factory builds up vertically, creating a "keep-up" series. During the late HST systems tract, the production rate exceeds the rate of relative sea-level rise, and series evolve into a phase coincident with a decrease in accommodation space. Restricted environments and subaerial exposure events become more common at the top of the thin upward-shallowing sequences. If the carbonate factory does not change, then the decrease in accommodation space relates to a thinning of the upward-shallowing sequences. Maximum sequence thicknesses occur toward the later stages of the TST systems tract and during the early HST systems tract, whereas minimum thicknesses occur during the initial stages of the TST systems tract and toward the end of the HST systems tract. If the carbonate factory changes at the end of the TST systems tract, parasequences thin because of the change in the biological community.

DEPOSITIONAL HISTORY OF WODEJEBATO GUYOT

Wodejebato is the most surveyed and best sampled guyot examined during Leg 144. The summit of Wodejebato Guyot is about 43 km long and increases in width from less than 12 km in the southeast to more than 25 km in the northwest. It is a four-lobated guyot with a "starfish" appearance and is covered by a carbonate platform. It has two perimeter ridges that lie along the shelves formed by the northern and northeastern flank ridge and along the ridge extending southeast toward Pikini Atoll (Bergersen, 1993). The flanks of the guyot may be divided into a steep upper slope (20°–24°) and a more gently inclined lower slope (about 7°); the transition depth between these two zones is about 2500 m. Five sites were drilled across the summit plateau (Fig. 1): one in the lagoon (Site 873), two on the inner perimeter ridge (Sites 874 and 877), and two on the outer perimeter ridge (Sites 875 and 876). Sites 873 and 874 were logged with the geophysical, geochemical, and Formation MicroScanner tool strings. Seismic data across the summit plateau varies in quality from a good six-channel profile to fair (but abundant) single-channel lines; the discussion in this manuscript focuses on the information obtained from the six-channel profile.

Formation of the Volcanic Platform

The $^{40}Ar/^{39}Ar$ radiometric ages for basalt recovered in the archipelagic apron sediments (Site 869; from 95.7 ± 0.3 Ma to 94.4 ± 0.3 Ma) and from the summit of Wodejebato (from 85.0 ± 1.5 Ma to 73.3 ± 3.6 Ma) show a long duration (~20 m.y.) of volcanism, which was not continuous in this area (Pringle and Duncan, this volume). Microfossil assemblages within the various volcaniclastic sediments on the summit plateau and in the archipelagic apron support these radiometric ages (Premoli Silva, Haggerty, Rack, et al., 1993; Shipboard Scientific Party, 1993). In the seismic data, the bright reflector at ~1.9 s two-way traveltime (TWT) and 2120 Z marks the acoustic basement (Fig. 2). This reflector probably relates to either volcanic flows or debris flows, and Bergersen (this volume) shows that acoustic basement shallows toward the center of the summit plateau to form a basement high (Fig. 2).

Erosion of the Volcanic Cone and the Formation of Carbonate Platform Setting

Erosion, weathering, and vegetative growth progressively modified the volcanic cone, transforming the summit into a gently sloping plateau with a central basement high (Figs. 2 and 3). The substrate sampled at sites across the summit plateau corresponds to a typical volcanic island weathering profile (Holmes, this volume). Altered

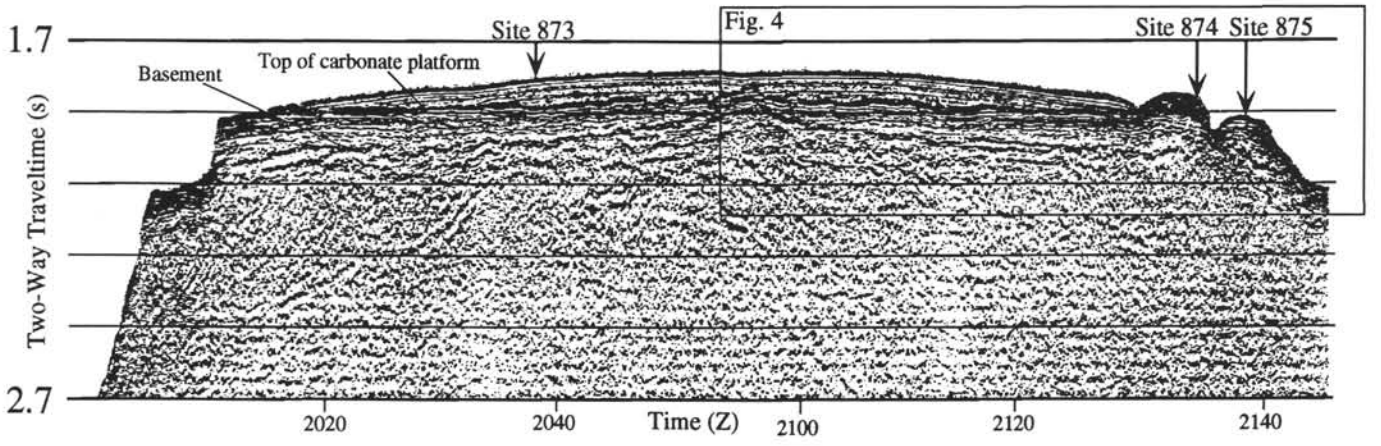

Figure 2. Migrated seismic profile (A–A′) on Wodejebato Guyot.

basalts (e.g., interval 144-873A-19R-3, 0–8 cm), claystone breccia (interval 144-877A-20R-4, 0–110 cm), and clays attest to the development of this weathering profile (Camoin et al., this volume). No such clays were recorded at Sites 875 and 876 on the outer perimeter ridge, where platform carbonates rest directly on basalt (Enos et al., this volume). The age estimate given by calcareous nannofossils from a black clay horizon interbedded at the bottom of carbonate sediments (interval 144-873A-11R-2, 18–22 cm) is late Campanian, around the *Radotruncana calcarata* Zone (Erba et al., this volume).

The clays dominating the weathering horizon presumably accumulated in erosional depressions. The low density and low velocity of this layer results in a strong acoustic impedance contrast between the overlying carbonates and the underlying volcanic breccia and flows. In the case of the carbonate to clay transition, the acoustic impedance transition is from high to low, resulting in a negative reflection coefficient. Hence, we interpret the negative polarity wavelet (i.e., the white interval) immediately above the seismic basement reflector as being related to the clay interval (Fig. 2). At some positions across the summit, this layer becomes too thin to be resolved in the seismic data.

Depositional History of the Carbonate Platform and Identification of Depositional Sequences

Timing and Paleontologic Characterization of Carbonate Depositional Sequences

The platform carbonates can be divided into four depositional sequences associated with five paleoecological assemblages (Premoli Silva et al., this volume).

1. Depositional Sequence I (DS-I). Paleoecological Assemblage V, dominated by abundant to common *Pseudorbitoides,* characterizes the first depositional sequence (Fig. 4). This very thin sequence (maximum thickness of ~20 m at Site 874) is late Campanian in age (Premoli Silva et al., this volume) and is present in lagoonal Site 873 and on the two inner perimeter ridge sites (874 and 877). DS-1 is missing in the two outer perimeter ridge sites (875 and 876; Fig. 1), although reworked *Pseudorbitoides* were recovered within a younger microfauna assemblage.

2. Depositional Sequence II (DS-II). Paleoecological Assemblages IV and III characterize this depositional sequence (Fig. 4). The most consistent components of Paleoecological Assemblage IV are rudists, corallinacean algae, and the abundant large benthic foraminifer *Sulcoperculina* and *Asterorbis,* associated with *Dicyclina* at Sites 873 and 874. In paleoecological Assemblage III, *Sulcoperculina* and *Asterorbis* (Pl. 3, Figs. 2–3, and Pl. 4, Figs. 1–2) alternate with a milolid-rich assemblage (Pl. 4, Fig. 3, and Pl. 5, Fig. 1), whereas a peculiar assemblage of *Istriloculina,* rotaliids, and discorbids represents the restricted marine environment (Pl. 5, Figs. 2–3). Diagnostic species are not abundant; consequently, it is difficult to estimate the age of these associations. DS-II appears, on the basis of strontium isotope analyses at Sites 874 and 877, to be Maastrichtian in age (Wilson et al., this volume). This sequence is present at Sites 873, 874, and 877, but it is represented as large, isolated intraclasts at the outer perimeter ridge sites (875 and 876; e.g., interval 144-875C-12M-2, 21–20 cm, and -13M-2, 67–72 cm; Premoli Silva, Haggerty, Rack, et al., 1993, p. 268). The thickness of DS-II varies from 60 m at Site 873 to 145 m at Site 877 (Fig. 4).

3. Depositional Sequence III (DS-III). Paleoecological Assemblage II and I at Sites 873, 874, and 877 and Subassemblages VIb, VIc, and VId at Sites 875 and 876 characterize this depositional sequence (Fig. 4). Abundant *Sulcoperculina* and *Asterorbis* associated with *Idalina* and *Vidalina* dominate paleoecological Assemblage II (recognized at Sites 873 and 877), whereas the occurrence of *Omphalocyclus* identifies paleoecological Assemblage I (recognized at Sites 873, 874, and 877). At the outer perimeter ridge sites (875 and 876), abundant *Sulcoperculina* and *Asterorbis,* associated with *Omphalocyclus,* characterize paleoecological Subassemblages VIb and VIc. DS-III is present everywhere on the guyot. At Sites 875 and 876, *Pseudorbitoides* are reworked at the bottom of the sequence. The thickness of DS-III varies from a maximum thickness of 85 m at Site 875 to a minimum thickness at the inner ridge and lagoon sites (<10 m at Site 874 and ~35 m at Site 873). The presence of *Omphalocyclus* and planktonic foraminifers of the *Gansserina gansseri* group indicates a Maastrichtian age, which is in agreement with strontium isotope values.

4. Depositional Sequence IV (DS-IV) is not easily distinguishable from DS-III. Paleoecological Subassemblage VIa, consisting of abundant *Asterorbis* and the absence of *Sulcoperculina* and *Omphalocyclus,* characterizes this sequence. The disappearance of *Sulcoperculina,* which was very abundant in the previous sequences, indicates that either an ecological event (e.g., climatic or temperature change) or a paleontologic event (e.g., turnover fauna) may explain this absence. DS-IV was observed only at outer perimeter ridge Sites 875 and 876; it has a maximum thickness of 85 m at Site 876.

Depositional Sequences, Sequence Boundaries, and Systems Tracts

Depositional sequences can be correlated to the lithologic units described by sedimentologists (Premoli Silva, Haggerty, Rack, et al., 1993, pp. 145–207).

1. At the bottom of the first depositional sequence, the top of the clay weathering horizon marks the first Sequence Boundary (SB)

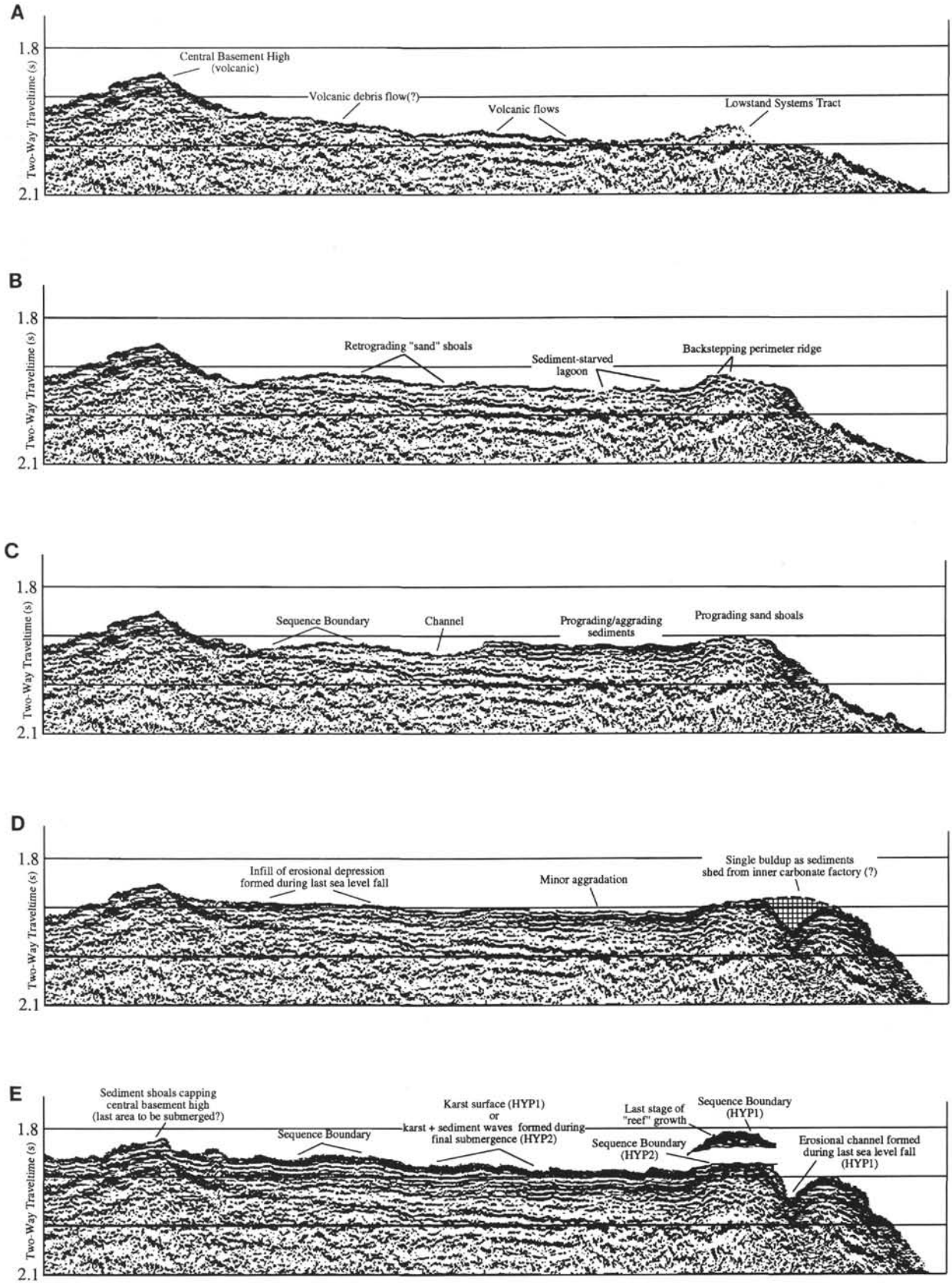

Figure 3. Depositional history of Wodejebato from the migrated seismic profile A–A′. **A.** Depositional Sequence I. A possible late lowstand (LST) or early transgressive (TST) systems tract exists on the platform edge. **B.** TST systems tract of Depositional Sequence II. **C.** Sequence boundary Ma1 truncating the previous HST systems tract of Depositional Sequence II. **D.** Last HST systems tract deposits of Depositional Sequence III. **E.** Erosional surface of Sequence boundary SB Ma2.

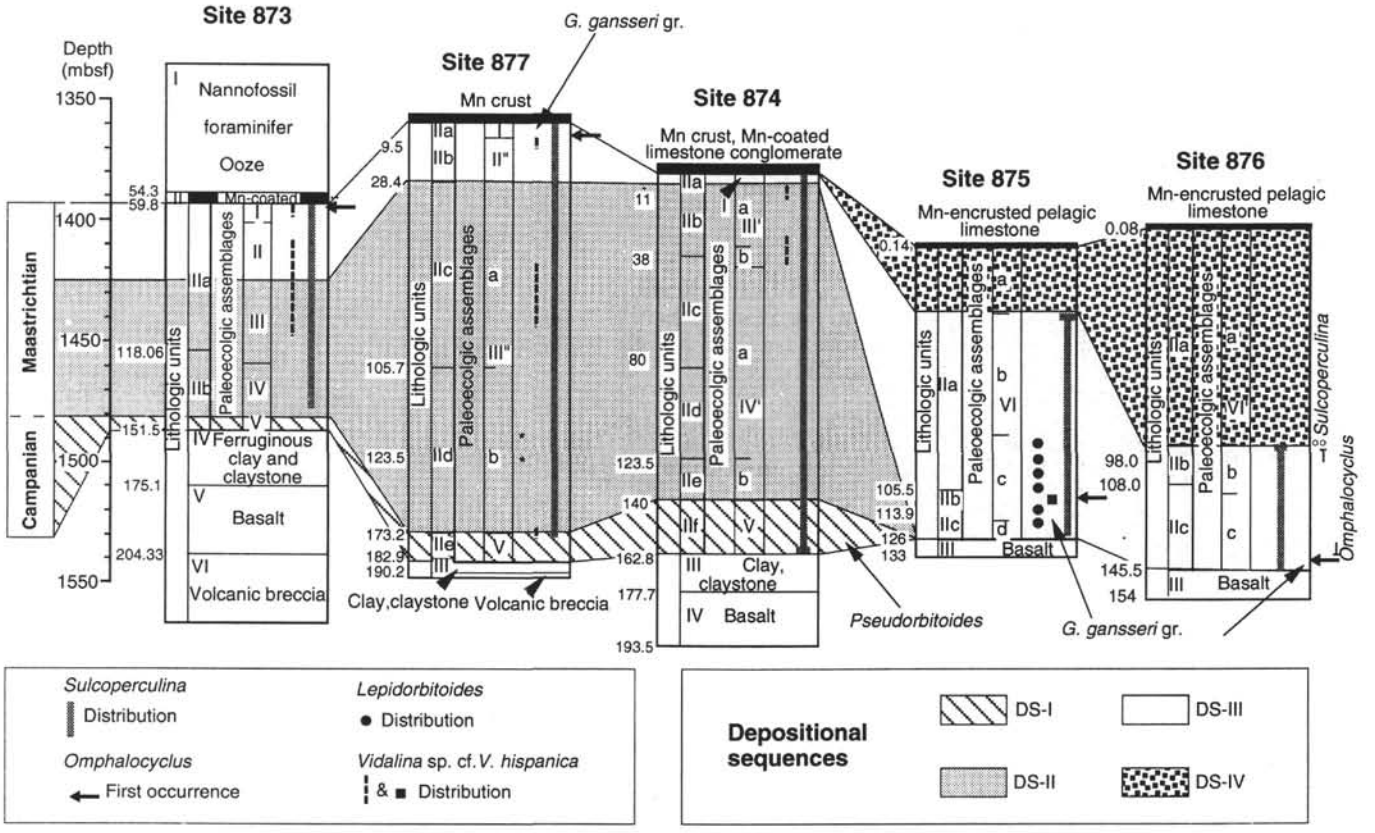

Figure 4. Depositional carbonate sequences of Sites 873 to 877 (modified from Premoli Silva et al., this volume).

Ca1. The distinctly different lithologic units across SB Ca1 produce a pronounced increase in resistivity (Hole 874B, Fig. 5; Camoin et al., this volume), but the thinness of the clay unit hinders identification of this boundary in the seismic data (Fig. 2). The age of SB Ca1 is probably late Campanian, close to the *R. calcarata* Zone identified in the overlying clay horizon (Erba et al., this volume).

2. DS-I (Sequence I, Fig. 4) is the thinnest sequence and corresponds to the colonization of the platform and early carbonate production. This sequence corresponds to Subunit IIB (partial) at Site 873 (lagoon, interval 144-873A-11R-2, 145 cm, to the bottom of Section 144-873A-10R-1); Subunit IIF at Site 874 (intervals 144-874B-20R-1, 23 cm, to -18R-1, 82 cm); and Subunit IIE at Site 877 (interval 144-877A-20R-1, 63 cm, to -19R-1, 27 cm; inner perimeter ridge). DS-I is very thin in the drill holes and hence unresolvable in the seismic data, although the true thickness of this unit in the lagoon is not known because the sites are located on the platform margin and near the central basement high. Consequently, the "white" interval above the seismic basement reflector may represent portions of DS-I in addition to the clay unit.

In the TST systems tract, the first marine carbonate bioclasts are interbedded or mixed with the topmost clays (4-mm-thick laminae of large benthic foraminifers in clays; Sample 144-874B-21R-1, 41 cm), presumably filling topographic depressions on the volcanic platform. The percentage of clay decreased as flooding of the platform progressed. The presence of calcareous nannofossils and planktonic foraminifers suggests a maximum flooding surface, above which an increased frequency of resistivity highs on well logs at Site 874 suggests a more restricted (shallower) environment up to the sequence boundary marked by a pronounced peak in resistivity (Fig. 5).

3. Basal SB Ca2 corresponds to the disappearance of *Pseudorbitoides.* A pronounced increase in resistivity marks the depth of SB Ca2 at Site 874 (Camoin et al., this volume). The occurrence of redeposited shallow-water clasts, foraminifers, and *Pseudorbitoides,* with more or less in situ planktonic foraminifers and calcareous nannofossils (assigned to CC22 Zone) in the archipelagic apron at Site 869, suggests that this sequence boundary probably also occurs in the late Campanian. The presence of a "questionable *G. aegyptiaca*" within these sediments (Shipboard Scientific Party, 1993) may be used to date the sequence boundary as ~73 to 74 Ma (the approximate appearance level of *G. aegyptiaca;* Erba et al., this volume). According to the strontium isotope curve (Wilson et al., this volume), the flooding of the platform occurs at the base of the Maastrichtian.

4. DS-II (Sequence II; Fig. 4) is the best documented sequence in the well-log, sedimentologic, biostratigraphic, and seismic data. This sequence is recorded in the lagoon (interval from the bottom of Sections 144-873A-10R-1, 120 cm, to -5R-1, 22 cm) and at the inner ridge (interval 144-874B-18R-1, 82 cm, to -2R-1, 25 cm, and interval 144-877A-19R-1, 27 cm, to -3R-1, 28 cm). It corresponds to lithologic Subunits IIIB (partial) to IIIA at Site 873, Subunits IIE to IIB at Site 874, and Subunits IID to IIC at Site 877. We recognized probable LST, TST, and HST systems tracts.

Above this sequence, the first carbonate sediments are only visible at the inner perimeter ridge (Sites 874 and 877) and occur as clean bioclastic sands (Pl. 1, Fig. 1). These sands are very poorly cemented and consist of fragments of rudists, corallinacean algae, echinoids, and bivalves. Such large benthic foraminifers as *Asterorbis* and *Sulcoperculina* dominate the microfaunal assemblage. Thicknesses of the upward-shallowing parasequences are difficult to estimate because the quality of the Formation Microscanner (FMS) records is very poor. In the seismic data, these bioclastic sands may form the acoustically indistinct unit lying directly above the reflector interpreted as acoustic basement. These facies are not identified at Site 873 in the lagoon; hence, the sequence could be interpreted as either the top of an LST prograding wedge or the bottom of the TST systems tract (Fig. 5).

At Sites 874 and 877, facies change from the poorly cemented underlying sands to an algal-coral-rudist grainstone/rudstone with a

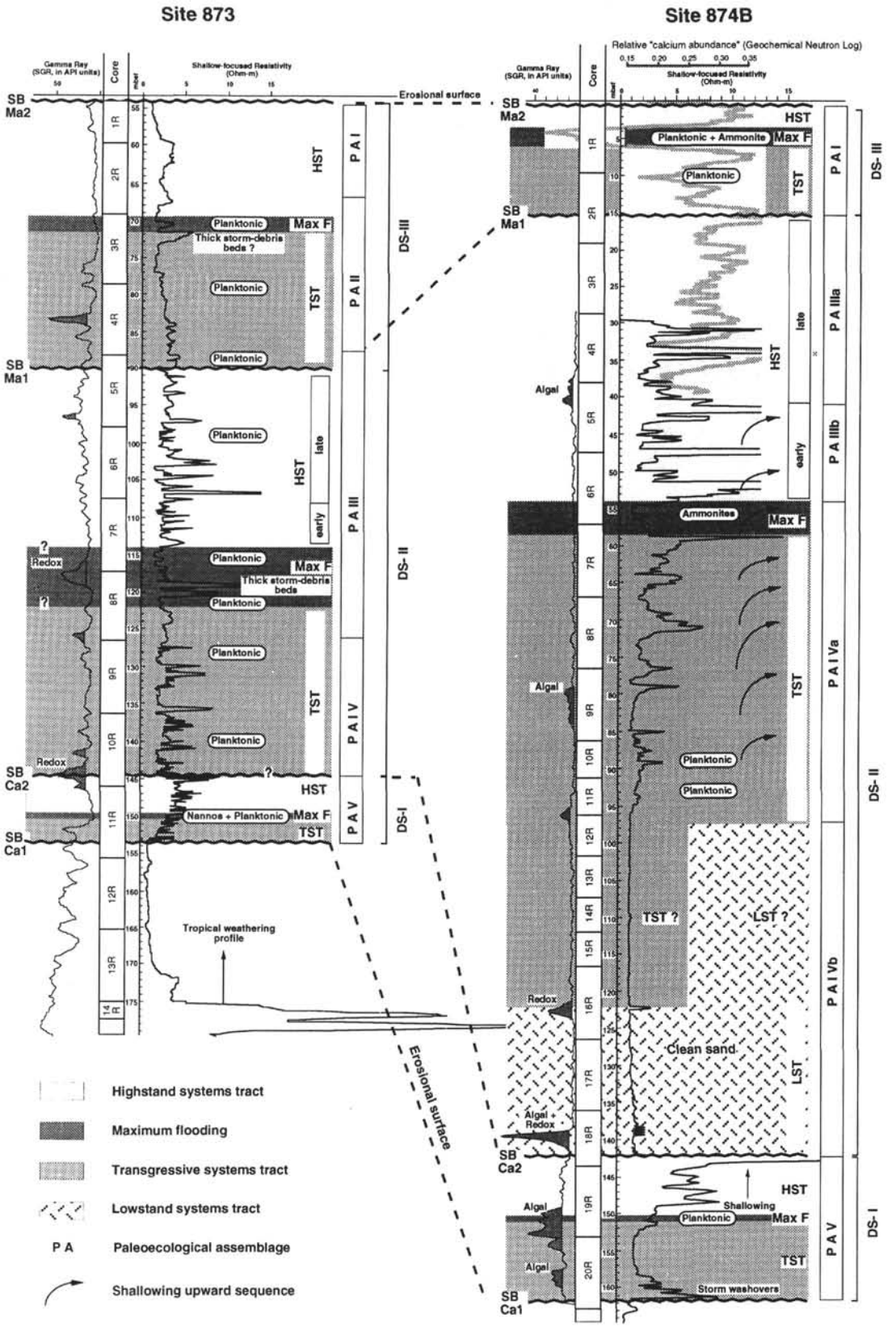

Figure 5. Formation MicroScanner, resistivity, and gamma-ray intensity well logs, interpreted sequences, and systems tracts of Sites 873 and 874, Wodejebato Guyot.

few algal-coral boundstones. The lack of recovery in Cores 144-874B-13R, -14R, and -15R makes it difficult to distinguish the boundary between the TST systems tract and the clean bioclastic sand unit. The FMS data are still poor over this interval, but peaks in natural-gamma intensity suggest two possible depths for the boundary (Fig. 5). Bioclastic facies usually correspond to poorly sorted skeletal grainstone and rudstone. Major skeletal components include rudists, corallinacean algae, corals, and echinoid fragments (Pl. 1, Fig. 2). The large benthic foraminifer *Asterorbis* decreases in abundance relative to the underlying bioclastic sand unit (Pl. 1, Fig. 3). The microfauna become more diversified from the bottom to the top of the TST, and species characterizing fully marine environments (e.g., nodosariids and *Marssonella*) become more abundant (Fig. 6). Few planktonic foraminifers were found in this unit; small ammonites at Site 874 mark the maximum flooding surface (Fig. 5 and Pl. 2, Fig. 1). On the basis of the well-log data, we identified six major cycles characterized by a progressive upward increase in resistivity (Fig. 5). In the seismic data, we interpreted the series of retrogradational reflectors as representative of an episode of carbonate factory backstepping (and associated landward retreat of the sand shoals) onto the central basement high (Fig. 3).

In the lagoon (Site 873), facies consist of skeletal grainstones, packstones, or wackestones with echinoid, rudist, and bivalve fragments, sparse corallinacean algae fragments, and ostracods (Fig. 6). The large benthic foraminifers *Sulcoperculina* and *Asterorbis* become rare (Pl. 2, Fig. 2) and a new flat species (*Dicyclina*) appears (Fig. 6 and Pl. 2, Fig. 3). Textulariids and rotaliids become more common. Close to the maximum flooding surface, green algae such as *Salpingoporella* and *Terquemella* are common (Pl. 3, Fig. 1); a peak in the abundance of planktonic foraminifers marks this surface.

The differences in microfaunal assemblages and abundances between the lagoon and perimeter ridge sites illustrate different depositional environments. For example, large benthic foraminifers such as *Sulcoperculina* and *Asterorbis* lived on the perimeter of the platform (the outer shelf). The empty tests of these foraminifers were redeposited on the inner shelf and lagoon during storm events; consequently, their abundance decreases toward the central portions of the platform (e.g., Site 873). Conversely, *Dicyclina* is a small, flat species that lived on seagrass leaves growing in a low-energy environment. The maximum abundance of the latter foraminifers corresponds to intervals of maximum abundance of green algae fragments. However, one faunal assemblage characteristic appears in common between the lagoon site and the inner perimeter ridge sites: an increase of planktonic species and higher diversity marks the vicinity of the maximum flooding surface.

Early and late HST systems tracts can be distinguished in the well-log, sedimentologic, and microfaunal data. The HST systems tract starts from the maximum flooding surface and corresponds to a decrease in abundance of planktonic species. Planktonic foraminifers still exist in the HST systems tract but not in the abundance noted at the maximum flooding surface.

The early HST systems tract does not exceed 5–15 m in thickness. The early HST systems tract facies at the perimeter ridge sites are similar to the late TST systems tract facies; a rudist-coral algal framework dominates the facies (Pl. 3, Figs. 2–3). Two large upward-shallowing cycles, shown by fluctuations in resistivity, compose the early HST systems tract at Site 874 (Fig. 5). In the lagoon, the facies consist primarily of rudists, with dasycladacean algae and miliolids appearing toward the top of this systems tract (Fig. 7). On the outer ridge, as the carbonate factory was presumably in a "catch-up" phase of production, the physiography of Wodejebato may have resembled a modern-day Pacific atoll.

A relative increase in calcium abundance and continued cycles of resistivity mark the late HST systems tract (Fig. 5). Parasequence thickness decreases upward. The bottom of the parasequences at Sites 874 and 877, characterized by rudists, corallinacean algae, corals, and *Asterorbis* (Pl. 4, Fig. 1), show more open-marine conditions than are found at lagoonal Site 873 (Fig. 8 and Pl. 4, Figs. 2–3). Rudists, corallinacean algae, and *Sulcoperculina* are the open-marine fauna within the lagoon. The tops show more restricted environments, early lithification processes, and emergence. Lagoonal and peritidal deposits are ubiquitous. The facies representing more restricted marine environments, similar across the platform, are dominated by a gastropod-ostracod wackestone/mudstone (Pl. 5, Figs. 1–2); microfauna include abundant rotaliids, discorbids, and *Istriloculina* (interval 144-874B-3R-1, 19–22 cm; Fig. 8 and Pl. 5, Fig. 3). The presence of similar faunal assemblages representing restricted environments within the lagoon and along the perimeter of the summit plateau suggests that the relief across the platform was minimal (accommodation space relatively consistent across the platform). In the seismic data, the HST systems tract appears primarily aggradational, although progradation probably occurred once the carbonate factory was able to keep pace with sea level and begin building outward over its own deposits (Fig. 3).

5. The interpreted erosional surface truncating the HST systems tract appears to have removed the lagoonal portions of this systems tract (adjacent to the central basement high). SB Ma1 corresponds to the first occurrence of *Omphalocyclus* and to the end of a lagoonal facies unit and associated restricted marine environment. The absence of DS-II at outer perimeter ridge Sites 875 and 876 (represented only by a few large reworked intraclasts of the inner platform facies) could be related to a substantial fall in sea level and erosion of the platform edge. The resistivity and gamma-ray logs at Site 873 do not show pronounced shifts across the proposed depth of this sequence boundary, nor do petrophysical properties change substantially. The relative "calcium abundance" curve at Site 874 increases at the level of the sequence boundary and shows an overall trend to less calcium abundance upward. Dolomitic beds below the proposed depth of SB Ma1 (interval 144-874B-2R-2, 47–55 cm; Camoin et al., this volume) may be related to emergence. The age of this sequence boundary is assigned to the Maastrichtian because DS-III yields *Omphalocyclus* and planktonic specimens of the *G. gansseri* group (Premoli Silva et al., this volume).

6. DS-III (Sequence III; Fig. 4) has been identified across the entire platform, including the outer perimeter ridge. This sequence corresponds to lithologic Subunit IIIA (partial) at Site 873 (intervals 144-873A-5R-1, 22 cm, to -3R-1, 0 cm); Subunits IIB and IIA at Site 877 (intervals 144-877A-3R-1, 28 cm, to -1R-1, 8 cm); the top of Subunit IIA at Site 874 (intervals 144-874B-2R-1, 25 cm, to -1R-1, 18 cm); Subunit IIC, IIB, and IIA (partial) at Site 875 (intervals 144-875C-14M-1, 65 cm, to -5M-1, 131 cm); and Subunits IIC and IIB at Site 876 (intervals 144-876A-15R-1, 12 cm, to -10R-1, 32 cm). Sequence thicknesses vary from a minimum of ~30 m in the lagoon to a maximum of ~95 m at Site 875 on the outer perimeter ridge. Facies within the sequence also vary, but all show more open-marine conditions. Possible LST, TST, and HST systems tracts are recognizable in the well-log, sedimentologic, and microfaunal data.

The well-sorted bioclastic sand of DS-II is overlain by a porous skeletal grainstone/packstone of DS-III on the outer perimeter ridge (Sites 875 and 876). Skeletal components include subequal percentages of large benthic foraminifers (such as *Sulcoperculina, Asterorbis,* and *Omphalocyclus),* mollusks (rudists, bivalves), echinoids, and corallinacean algae fragments (Enos et al., this volume). At the bottom of the holes, large intraclasts of muddy packstone and *Pseudorbitoides* are mixed within the bioclastic sand; these packstones and single fossils were probably eroded and reworked from the top of the HST systems tracts of DS-II and DS-I, respectively. This interpreted reworking suggests that the subaerial erosion preceding DS-III reached the two underlying carbonate depositional sequences. The basal sand unit is also considered as a part of the late LST systems tract or the bottom of the TST systems tract.

Resolution of the seismic data precludes identification of the TST and HST stratal patterns in this depositional sequence; however, carbonate deposition was presumably aggradational after the central basement high was covered by sediments (Fig. 3). Facies in the

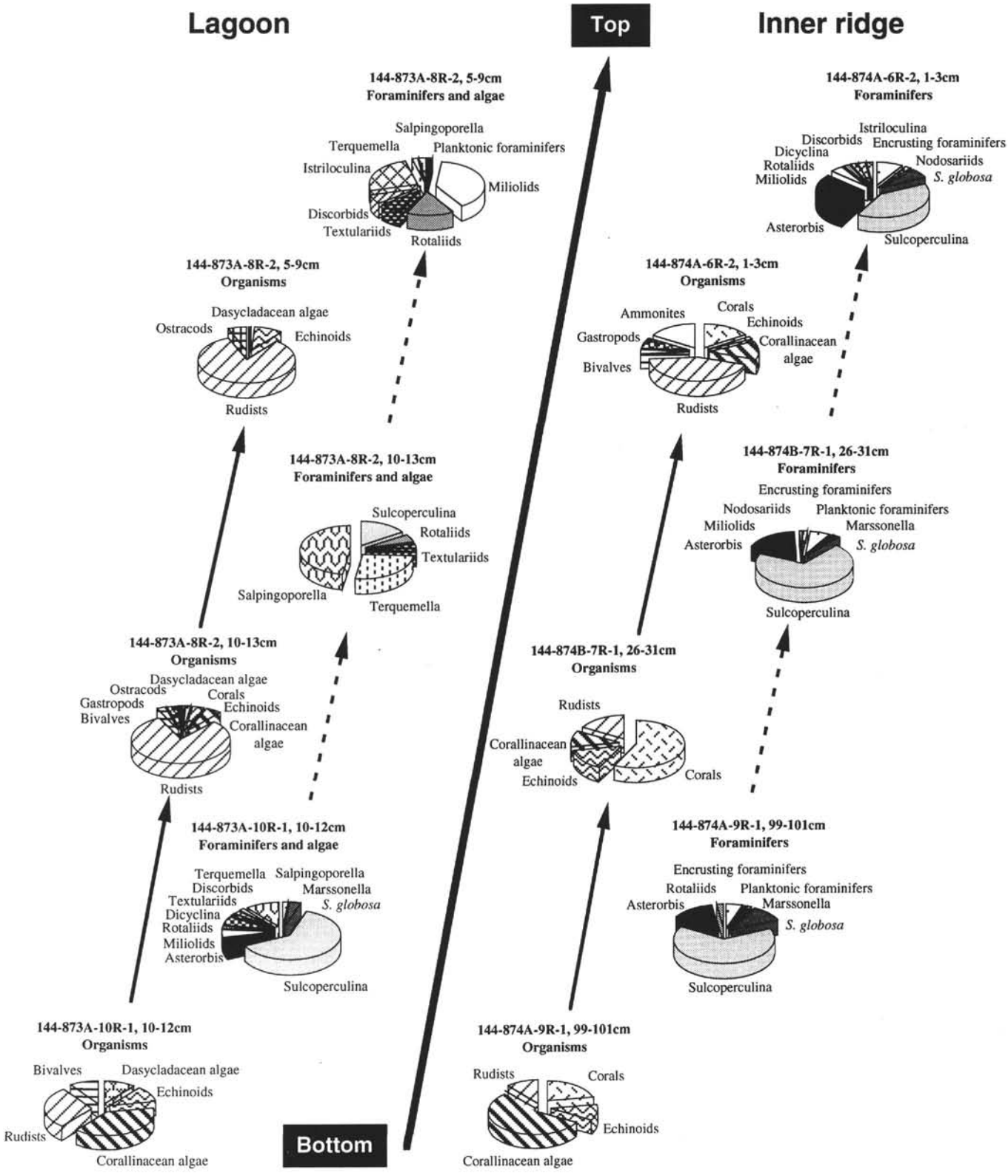

Figure 6. Biological content of the TST systems tract of Depositional Sequence II.

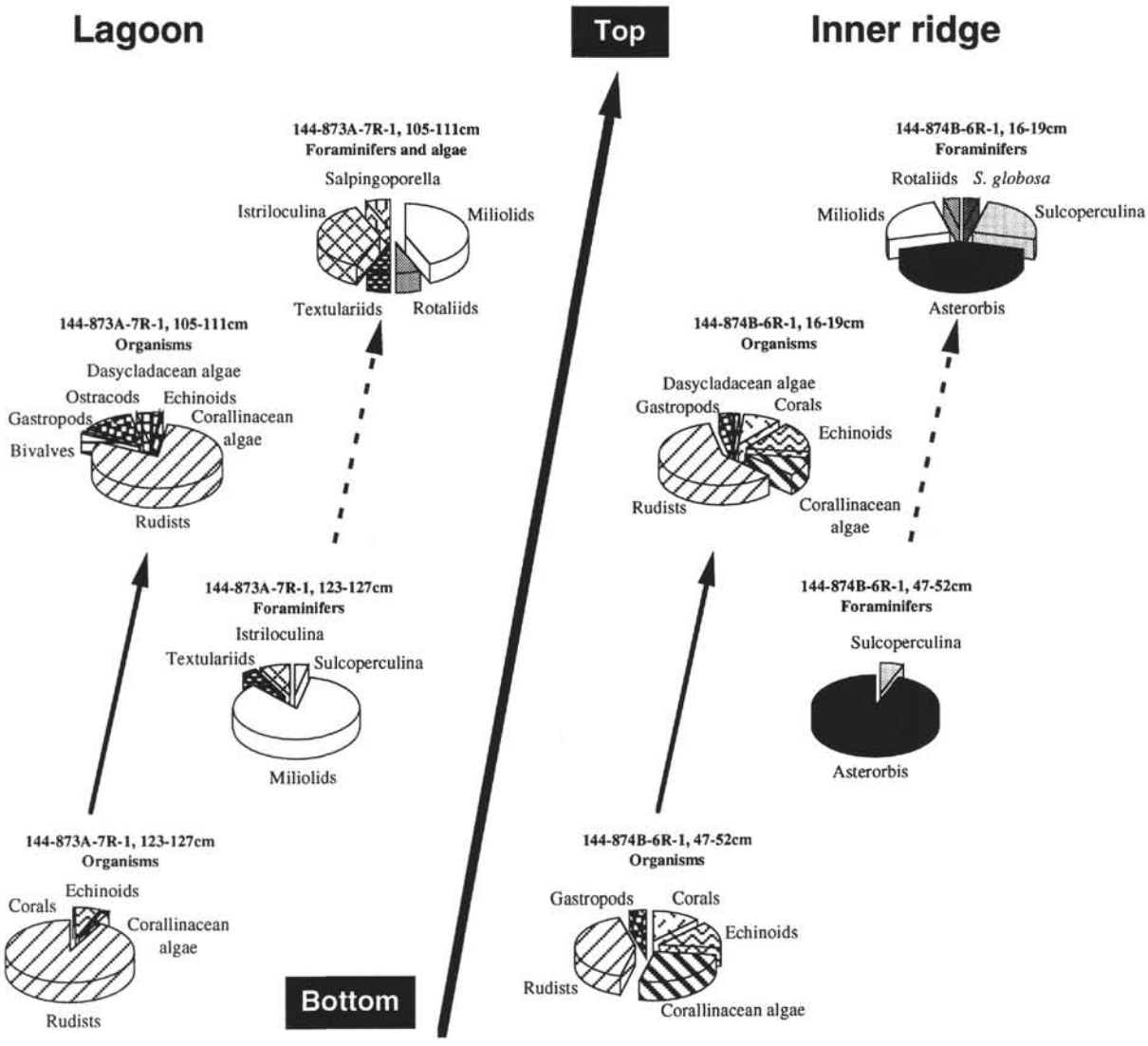

Figure 7. Biological content of upward-shallowing sequences in the early HST systems tract of Depositional Sequence II.

lagoon (Site 873) and at the inner perimeter ridge (Sites 874 and 877) are characterized by large rudists, suggesting that normal conditions of salinity and oxygenation existed across the entire platform. The presence of planktonic foraminifers marks the later stages of the TST systems tract, whereas the appearance of ammonites marks the maximum flooding surface (intervals 144-877A-4R-2, 18–21 cm, and -4R-3, 13–27 cm). In the well-log data, the maximum flooding surface corresponds to a depletion of calcium and a relative peak of resistivity at Site 873 (Fig. 5).

7. SB Ma2 is interpreted as a pronounced emergence surface. The presence of intraclasts of skeletal packstone and rudist fragments suggests a probable conglomerate at the top of Site 873 (Premoli Silva, Haggerty, Rack, et al., 1993, p. 638), and depleted ^{18}O values suggest a meteoric origin for aragonite-calcite replacements in sediments at Site 874 (Camoin et al., this volume). Recovery of a probable *Microcodium* also suggests soil formation at Site 874 (interval 144-874B-1R-1, 40–47 cm). Although echo-sounder profiles show relief across the platform top of only 5 to 10 m, the magnitude of this emersion can be inferred from the depth of karstic cavities (>50 m; interval 144-874B-6R-1, 0–4 cm) noted at Site 874. Maastrichtian planktonic foraminifers (interval 144-874B-3R-1, 114–118 cm) or Eocene–Paleocene planktonic foraminifers and calcareous nannofossils (Premoli Silva, Haggerty, Rack, et al., 1993, p. 229) fill these karst cavities. The age of the sequence boundary, as determined by planktonic foraminifers filling the karst cavities, is Maastrichtian. If our interpreted depth of karstification is correct, the sea-level fall associated with this emergence was a major event.

8. DS-IV (Sequence IV; Fig. 4) is the last carbonate platform sequence deposited and is only identified at the outer perimeter ridge (Sites 875 and 876). This sequence corresponds to lithologic Subunit IIA at Site 875 (intervals 144-875C-5M-1, 131 cm, to -1M-1, 7 cm) and Site 876 (intervals 144-876A-10R-1, 32 cm, to -1R-1, 10 cm). A manganese crust covers DS-IV, as well as DS-III on the inner perimeter ridge sites.

This sequence is a bioclastic calcarenite similar to the underlying bioclastic sand unit, but it has a higher porosity. An important difference between the two bioclastic units is the absence of *Sulcoperculina* and *Omphalocyclus* in DS-IV.

The sediments of DS-IV can be interpreted to be a "forced regressive wedge of a lowstand" or a unit consisting of high-energy grainstones lying conformably on the distal part of the previous highstand (Handford and Loucks, 1993; Jacquin and Vail, in press). The deposition of this youngest unit on the edge of the platform and at a topographic level lower than the top of the platform supports the hypothesis that the sands were deposited during a fall in sea level (and hence are the LST), whereas the inner part was exposed and karstified. The

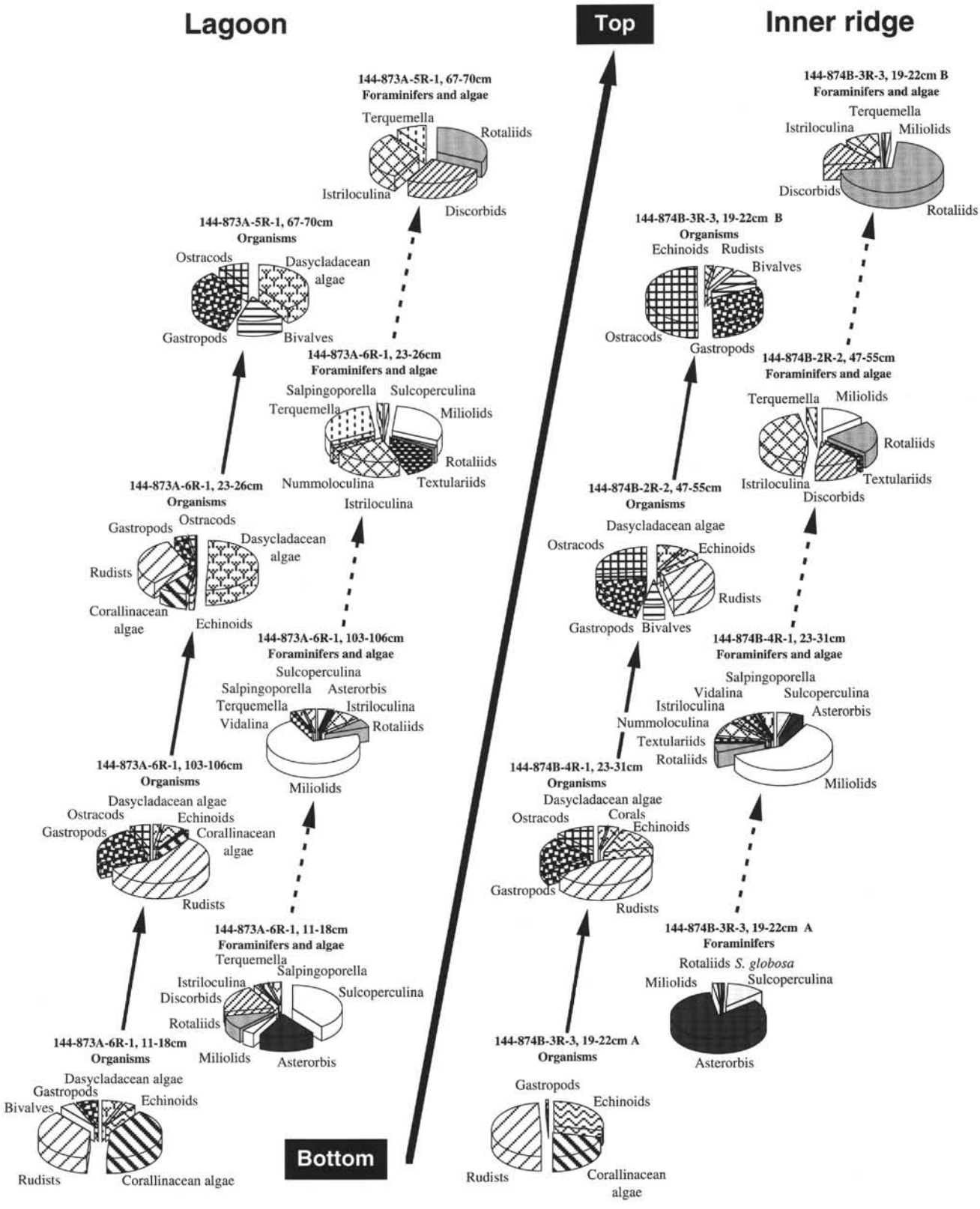

Figure 8. Biological content of upward-shallowing sequences in the early HST systems tract of Depositional Sequence II.

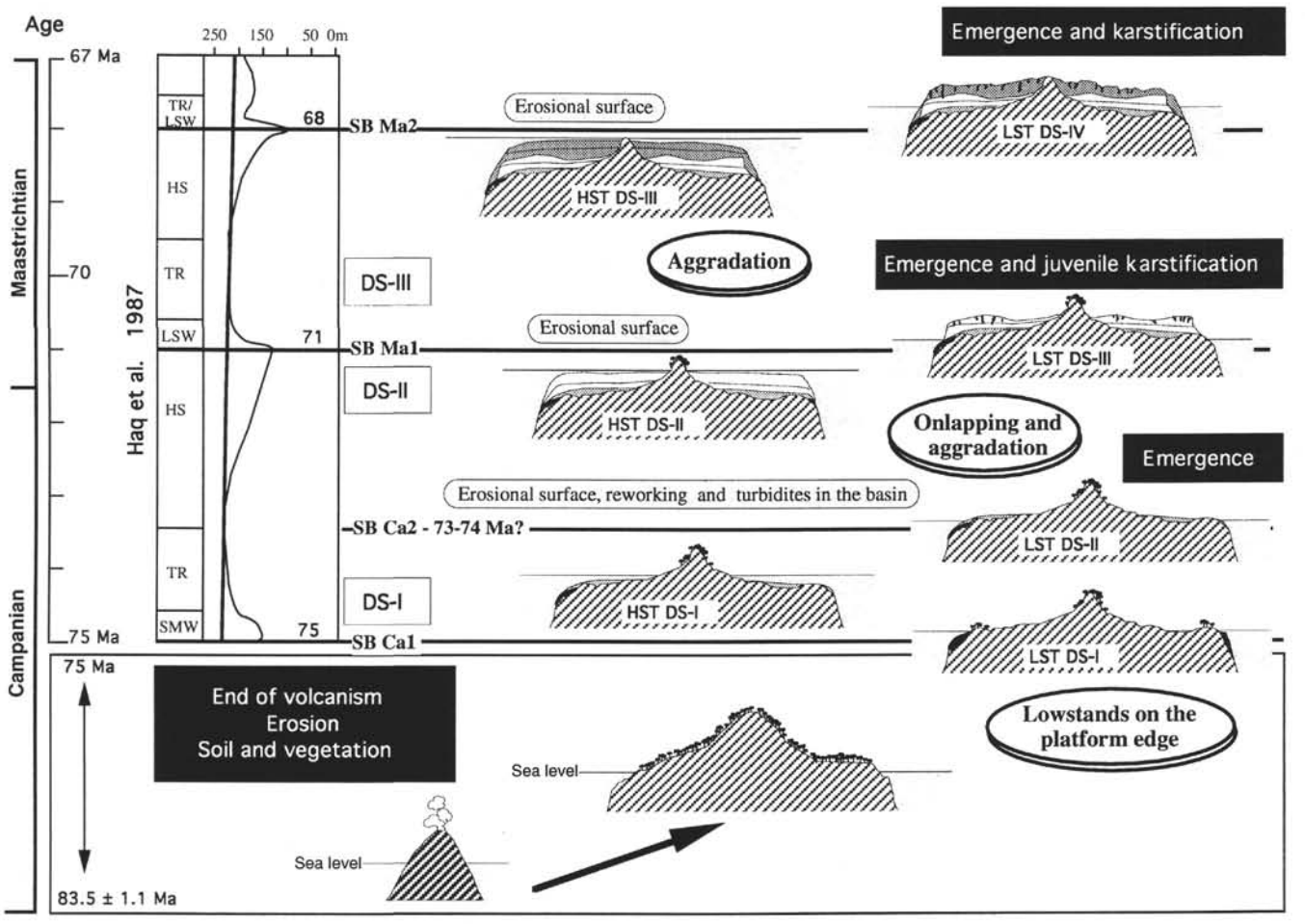

Figure 9. Summarized evolution of a small, mid-ocean carbonate platform, Wodejebato Guyot.

hypothetical TST and HST systems tracts succeeding the LST systems tract are not recorded by shallow-water carbonate sediments; rather, a manganese crust covers the failure surface of this platform.

Conclusions

Figure 9 summarizes the evolution of depositional environments on Wodejebato Guyot. After the transformation of the volcanic island to a platform suitable for carbonate accumulation, four identifiable carbonate depositional sequences accumulated on top of the platform. Three of the sequence boundaries can be tentatively related to the 68, 71, and 75 Ma sea-level lows on the Haq et al. (1987) sea-level curve; our SB Ca2 (~73-74 Ma) is not shown on this curve.

The resolution of the existing seismic data limit the degree to which stratal patterns can be used to identify depositional sequences and systems tracts. During the initial depositional sequences when the central basement high remains uncovered by sediments, retrogradational reflectors mark periods of relative sea-level rise and backstepping of the carbonate factory. During sea-level highstands, the carbonate factory can prograde over the existing sediments. After further development of the platform and burial of the central basement high, carbonate deposition becomes principally aggradational (Fig. 3). Distinct sequence boundaries are difficult to identify on the seismic profiles, although we interpret the reflectors as marking the top of the volcanic platform (SB Ca1), the top of DS-II (SB Ma1), and the top of the carbonate platform (SB Ma2).

Reworked sediments are present at the bottom of each sequence. Wood and weathered volcanic fragments occur at the bottom of DS-I, *Pseudorbitoides* lie at the bottom of DS-II, and reworked *Pseudorbitoides* and carbonate clasts of DS-II are found at the bottom of DS-III. Coarse, poorly cemented bioclastic sands compose the late LST systems tract (or the early TST systems tract), whereas planktonic foraminifers and, occasionally, ammonites mark the TST systems tract. These microfossils become more abundant close to the maximum flooding surface, where they are associated with species marking fully marine environments (e.g., nodosariids and *Marssonella*). Conversely, the late HST systems tract shows the most restricted environments across the entire platform.

We suggest that a major fall in sea level occurred before final platform submergence. DS-IV at the outer perimeter sites consists of a unit interpreted as a "forced regressive wedge of a lowstand." Neither the TST nor the HST systems tracts of this sequence were recovered by drilling or dredging. The absence of transitional sediments between the last shallow-water carbonate deposits and the pelagic sediments filling the karstic cavities suggests either a relatively rapid and large rise in sea level or a change in environmental conditions such that the carbonate factory could not keep pace or catch up after sea level became more stable.

DEPOSITIONAL AND EROSIONAL HISTORY OF LIMALOK GUYOT

Limalok (formerly Harrie) Guyot is located in the southern part of Marshall Islands (5.6°N, 172.3°E; 53.7 km from Mili Atoll in the Ratak Chain; see site map preceding title page). This "tongue-shaped" island is about 47.5 km long and increases in width from less

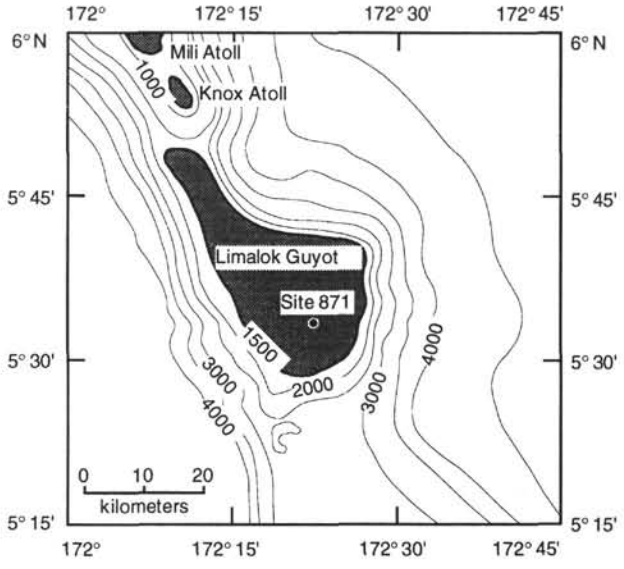

Figure 10. Areal distribution of the carbonate platform of Limalok Guyot (Site 871).

than 5 km in the northwest to more than 24 km in the southeast (Fig. 10). The carbonate platform was recovered at central Site 871. The relative paucity and poor quality of drilling and seismic data hamper interpretations of the carbonate deposition on Limalok Guyot: only one lagoonal site was drilled and only single-channel seismic profiles cross the summit plateau. Nonetheless, enough information exists to attempt placing the gross depositional history of this platform into a sequence stratigraphy framework.

Formation and Erosion of the Volcanic Platform

No $^{40}Ar/^{39}Ar$ dates exist for the basalt and clasts of basalt recovered from the volcanic platform. The overlying variegated clays of lithologic Subunits IIIC and IIIB may represent a soil horizon developed under tropical weathering conditions (Premoli Silva, Haggerty, Rack, et al., 1993, pp. 41–103; Holmes, this volume). Similar to Wodejebato Guyot, the first carbonate sediments were deposited on this soil horizon.

Depositional History of the Carbonate Platform and Identification of Systems Tracts

Timing and Paleontologic Characterization of Carbonate Depositional Sequences

We divided the carbonate platform into a minimum of four depositional sequences, ranging from the latest Paleocene to the earliest middle Eocene.

1. Depositional Sequence A (DS-A) (from 425.7 to 410 or 387.6 mbsf). Paleoecological Subassemblage IIIc and part of Subassemblage IIIb, dominated by red algae occurring as rhodoliths, characterize DS-A (Fig. 11). The occurrence of *Alveolina* sp. in the basal carbonate unit of Section 144-871C-32R-1 constrains the age of this unit to planktonic foraminifer Zone P5 and nannofossil Zone CP8, or the latest Paleocene (~55 Ma; Nicora et al., this volume). Alternatively, Watkins et al. (this volume), on the basis of calcareous nannofossils found in intervals 144-871C-32R-1, 10–90 cm, and -31R-1, 47–48 cm, suggest that the first carbonate sediments were deposited in the latest Paleocene (Zone CP5, ~58.5 Ma; Okada and Bukry, 1980).

2. Depositional Sequence B (DS-B) (from 410 or 387.6 to 322 or 331.5 mbsf). Paleoecological Subassemblages IIIb and IIIa characterize DS-B. Red algae are the dominant components of this assemblage, but dasycladacean algae are also well represented. The large benthic foraminifer *Discocyclina* disappears at the top of this sequence. *Asterocyclina* sp. occurring in Samples 144-871C-29R-1, 16–21 cm, and -29R-1, 7–13 cm, indicates an early Eocene age (middle Illerdian) for this unit. Species of *Nummulites* and *Aveolina* (*Glomalveolina*) range from the basal to the middle of the middle Illerdian. Consequently, to be consistent with other data from DS-B, this sequence begins in the early Eocene or the latest Paleocene (~54 Ma) and finishes probably before the middle early Eocene (~51.5 Ma).

3. Depositional Sequence C (DS-C) (from 322 or 331.5 to 161.7 or 152.9 mbsf). Paleoecological Assemblage II characterizes DS-C. Species within this sequence are diagnostic of lagoonal environments. At the base are reworked clasts, and abraded foraminifers form paleoecological Subassemblage IIc. Alveolinids dominate paleoecological Subassemblage IIb, whereas abundant miliolids in the absence of large foraminifers (a typical lagoonal assemblage) characterize paleoecological Subassemblage IIa. The presence of *Alveolina ilerdensis* (Sample 144-871C-20R-1, 113–118 cm) suggests that the base of the sequence cannot be older than the middle to upper part of the middle Illerdian (early Eocene). Higher in the sequence (Sample 144-871C-15R-1, 15–20 cm), the presence of *Alveolina pinguis* indicates the middle to upper Cuisan (middle to late early Eocene age). This age assignment is consistent with the presence in Sample 144-871C-8R-1, 21–25 cm, of a few specimens of the *Guembelitrioides higginsi* group, which ranges from the base of Zone P9 (upper lower Eocene) to Zone P11 (lower middle Eocene). Consequently, this sequence ranges in age from middle early Eocene to late early Eocene. Poor recovery and the associated paucity of paleontologic controls prevented further subdivision of this very thick sequence, which is probably composed of two or more sequences (Ogg et al., this volume).

4. Depositional Sequence D (DS-D) (from 161.7 or 152.9 to 140.8 mbsf). Paleoecological Assemblage I characterizes DS-D. Large foraminifers such as "pillared" *Nummulites* are common, in addition to *Coleiconus elongatus* and large miliolids. The appearance of *N. laevigatus* in Core 144-871C-2R identifies the *Nummulites laevigatus* Zone, making this sequence early middle Eocene in age.

Depositional Sequences and Systems Tract

1. Similar to that of Wodejebato, the first sequence boundary (SB-A) is located between the volcanic substrate and the initial carbonate platform sediments (Fig. 12). SB-A is seen in the seismic profiles as a strong reflector at ~2.0 s TWT on the south side of guyot, shallowing to ~1.52 s TWT toward the center of the summit plateau (Fig. 13). The considerable relief observed along this reflector possibly represents small incised valleys across the volcanic platform. Small carbonate shells of gastropods represent the first carbonate deposits overlying this sequence boundary (Premoli Silva, Haggerty, Rack, et al., 1993, pp. 41–103).

2. The branch-, ball-, and carpet-shaped red algae dominating DS-A characterize the colonization of the volcanic platform during the initial transgressive sea-level phase. These diverse forms suggest that the red algae occupied all ecological niches and hence were able to tolerate a wide range of clay and nutrient fluxes. The sediments of this sequence may represent either a single episode of flooding (maximum flooding surface around 410 and 415 mbsf, indicated by low resistivity and the presence of nannofossils) or a pair of sea-level transgressions (with the second maximum flooding surface around 395 mbsf, also associated with a low-resistivity peak). Depending on the position of SB-B, the thickness of DS-A at Site 871 is between 15 and 35 m, neither of which can be resolved by the seismic data.

3. We are uncertain where to place the second sequence boundary (SB-B). Two possibilities exist: at the end of paleoecological Subassemblage IIIc near the probable Paleocene/Eocene boundary or at the end of the rhodolith assemblage (paleoecological Subassemblage IIIb)

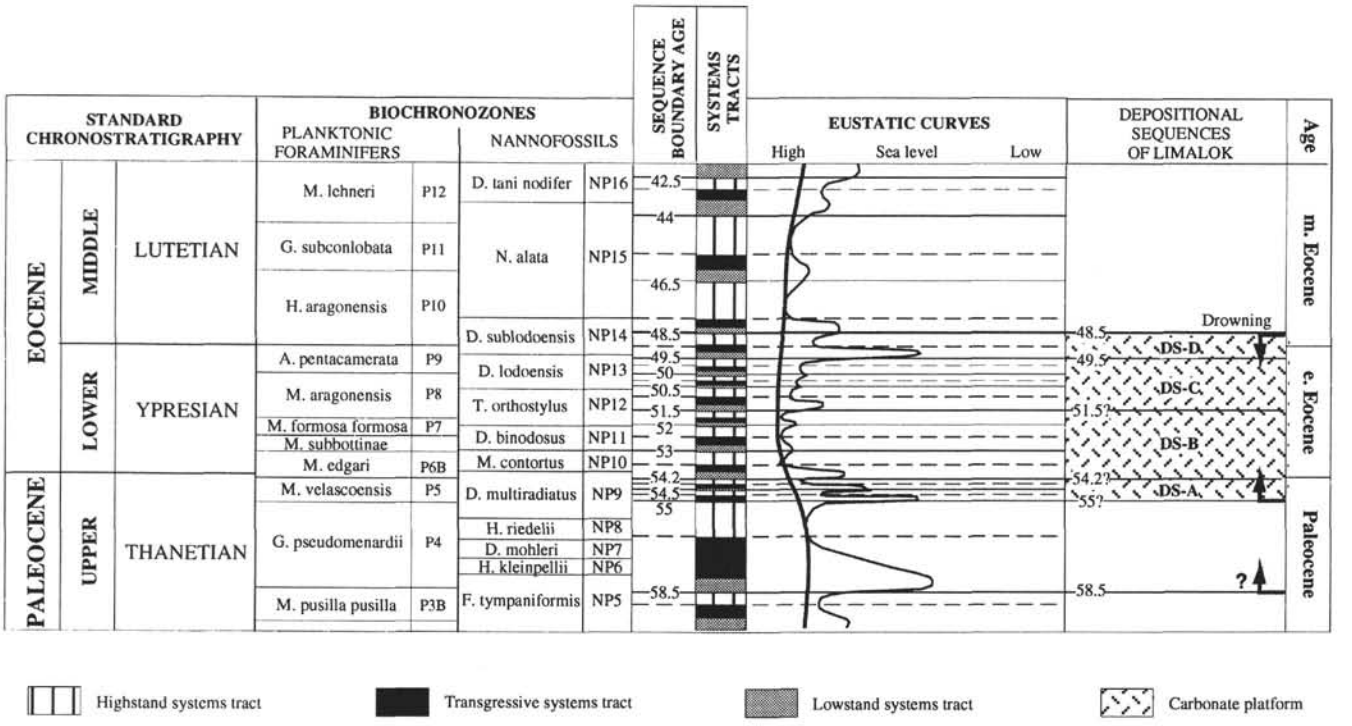

Figure 11. Depositional sequences at Limalok according to the Haq et al. (1987) chart of sea-level change.

in the earliest Eocene. In the well-log data, a resistivity peak marks the Paleocene/Eocene boundary (around 410 mbsf), whereas an overall decrease in resistivity corresponds to the disappearance of the rhodolith assemblage (around 387.6 mbsf, Fig. 12; Ogg et al., this volume).

4. Ogg et al. (this volume), on the basis of well-log information, list several possible hypotheses for the sediments of DS-B, but the poor recovery throughout this interval prevented us from confirming any of them. The maximum flooding surface is documented by the presence of planktonic foraminifers (Sample 144-871C-24R-1, 0–4 cm) and is located around 355 mbsf.

5. SB-C corresponds to the disappearance of *Discocyclina.* The presence of reworked clasts and foraminifers immediately above the proposed sequence boundary suggests subaerial exposure and erosion. Stratigraphically, the sequence boundary separates the early early Eocene and the middle early Eocene depositional sequences. On the basis of the well-log data, the best position for this sequence boundary is either beneath the zone of resistivity and gamma-ray peaks or above the more subdued resistivity and gamma-ray curves (Fig. 12). SB-C may correlate with the toplap surface described by Bergersen et al. (1992).

6. DS-C corresponds to the end of red algae domination and the beginning of lagoonal deposition. At the bottom of DS-C, reworked sediments are overlain by quiet-water faunal assemblages (e.g., alveolinids). The presence of planktonic foraminifers in Sample 144-871C-8R-1, 21–25 cm, documents a maximum flooding surface. Above the maximum flooding surface, the presence of shallow-water and beach facies suggests a shallow-marine environment subject to periodic emergence.

7. SB-D corresponds to the end of quiet depositional conditions (i.e., lagoonal), as shown by an absence of large benthic foraminifers. Above the sequence boundary, the appearance of large benthic foraminifers, along with a turnover in fauna, suggests a more open-marine environment. The sequence boundary separates early and middle Eocene deposits. In the well-log data, either the last peak in resistivity or the last peak in gamma intensity marks the sequence boundary (Fig. 12).

8. DS-D indicates a more open-marine lagoonal environment, as shown by the occurrence of large benthic foraminifers such as *Nummulites* and orbitolinids. The maximum flooding surface is suggested around 147 mbsf by the low resistivity, but this has not been documented by the planktonic foraminifers.

9. SB-E corresponds to the demise of the carbonate platform. A manganese-phosphatic crust coating SB-E yields a nannofossil assemblage attributed to Zone CP13 of middle middle Eocene age.

Summary

The depositional history of Limalok Guyot is probably more complex than outlined here, but the relatively poor data quality prevents a more detailed interpretation. On Figure 11, the sequence boundaries can be tentatively related to sea-level lows on the Haq et al. (1987) curve. SB-A may correspond to either 58.5 or 55 Ma. The poor data quality of SB-B precludes assigning one particular low shown in Haq et al. (1987), but three sea-level lows (55, 54.5, and 54.2 Ma) are possible within this time frame (Fig. 11). The curve shows a major fall in sea level at 51.5 Ma, but smaller amplitude fluctuations exist below (52 and 53 Ma) and above (50.5 Ma), and one of them may correspond to SB-C. SB-D and SB-E may be related to ~49.5 and 48.5 Ma.

CONCLUSIONS

The relatively small size and thickness of these mid-ocean platforms, along with their isolation from external terrigenous sources, requires that the sequence stratigraphy model be modified to fit the physical realities of these depositional environments. On both Wodejebato and Limalok guyots, the following observations can be made: (1) the volcanic cone was eroded and weathered to such a degree that a relatively flat volcanic platform existed before the first shallow-water carbonates were deposited; (2) the carbonate depositional units initially onlapped the central basement high and became more aggradational as this high was covered by sediment; (3) a true lagoon appears

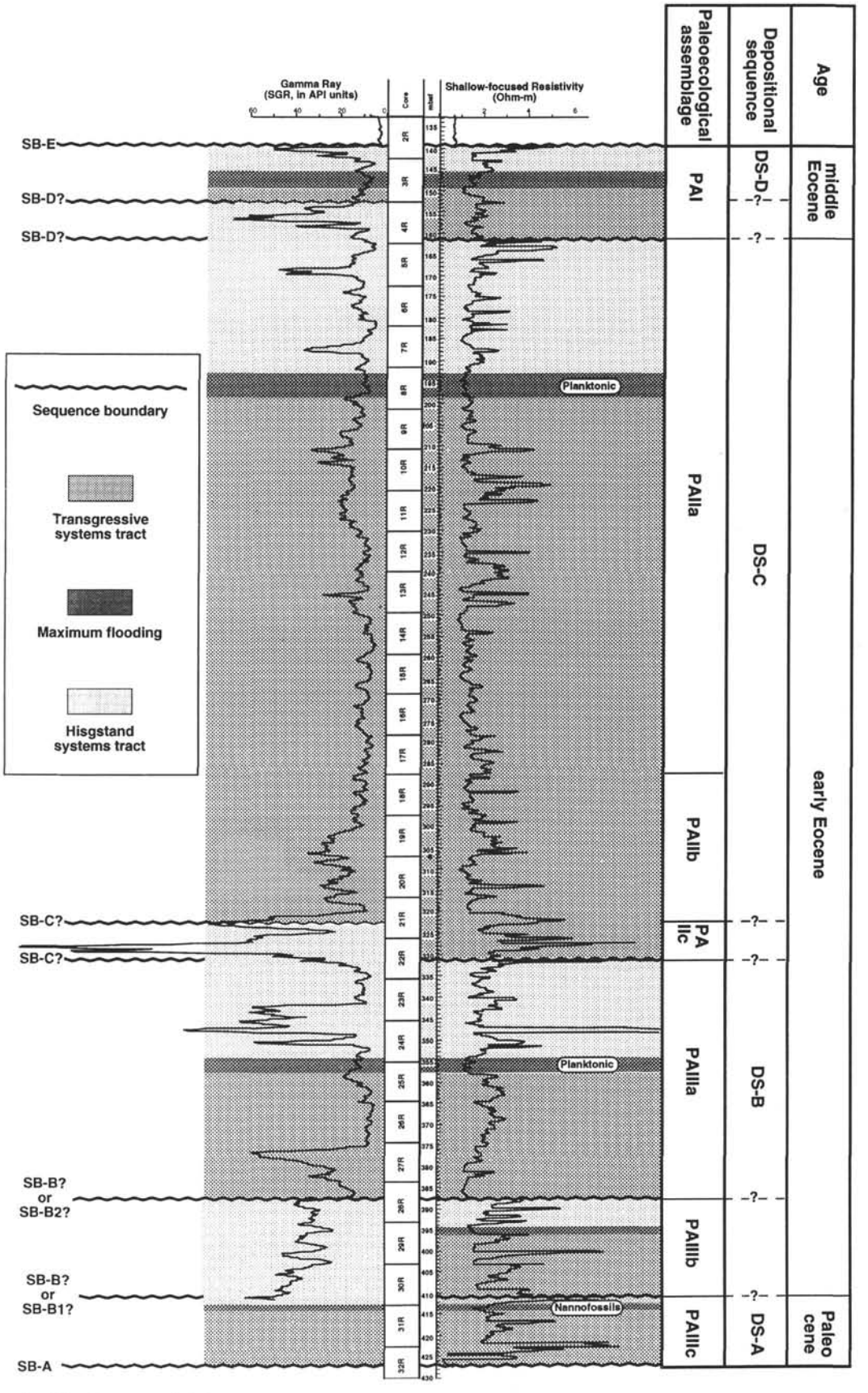

Figure 12. Formation MicroScanner, resistivity, and gamma-ray intensity well logs, interpreted sequences, and systems tracts of Site 871, Limalok Guyot.

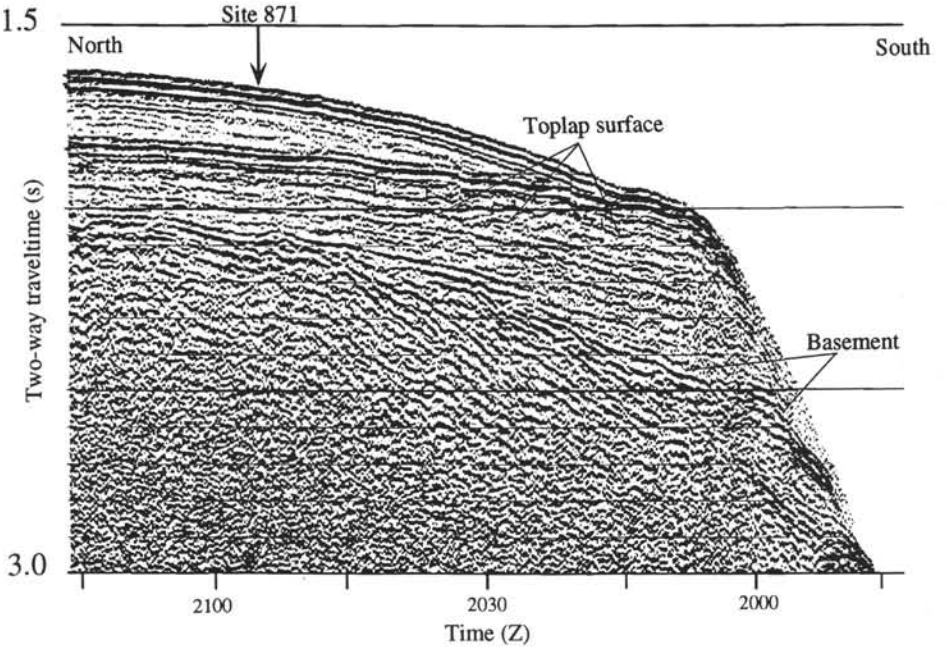

Figure 13. Seismic profile of Limalok Guyot.

when the sediment setting becomes more flatter; (4) planktonic foraminifers or ammonites mark the maximum flooding surfaces; (5) a minimum of four depositional sequences separated by probable emersion surfaces exist across the platforms; and (6) no transitional sediments marking the demise of the platform exist between the shallow-water carbonates and the overlying pelagic sediment.

During the Cretaceous, Wodejebato and Limalok were broad shield volcanoes related to hotspot activity probably near French Polynesia (Lincoln et al., 1993; Bergersen, this volume). Cooling and subsidence of the plate as it moved away from the region of active volcanism resulted in erosion, partial truncation, and expansion of the shelf margin, providing the initial depositional setting for the sediments drilled during Leg 144. Alteration of volcanic products formed a clay weathering profile, upon which vegetation grew and red algae colonized. The clay/carbonate contact represents the first sequence boundary on these guyots.

The first carbonate sediments on these volcanic platforms accumulated near the shelf margin, with the initial depositional setting being a gently inclined clay-rich volcanic platform shallowing toward a central basement high. The ability to discern these "buildups" in seismic profiles depends on such factors as the frequency of the seismic source, the number of channels of data collected, the depth of acoustic penetration, and the thickness of the sediment units. Neither of the basal depositional sequences identified on Wodejebato and Limalok (on the basis of lithology, faunal assemblages, and well-log data) are visible in the seismic data presented in this paper because of a combination of the above-listed factors. Rather, in the six-channel seismic data over Wodejebato Guyot, we see two principal stratal patterns related to the first major sea-level transgression across the volcanic platform (Fig. 14C). First, the carbonate factory, which was established along the perimeter of the summit plateau, fails to keep up with the rapidly rising sea level. This rapid upward growth along the shelf margin creates an "empty bucket" type atoll morphology with a raised perimeter ridge and sediment starved lagoon. Second, as the carbonate factory fails along the summit plateau margin, the zone of carbonate production backsteps onto the gently sloping volcanic platform. Such backstepping is visible in the seismic data as a series of stacked, retrogradational shoal units with reflectors truncating against the basement reflector. These retrogradational units backstep until carbonate sediment production keeps pace with the rise in sea level, and form the major transgressive units (the TSTs) on both Wodejebato and Limalok.

As sea level stabilizes with the central basement high still emergent, the carbonate sediments begin to aggrade and prograde, marking the beginning of the HST systems tract (Fig. 14C). The carbonate factory progrades seaward toward the shelf margin and the carbonate sediments aggrade to sea level, resulting in a slowing of sediment production. Minor changes in sea level can cause seaward or landward shifts in the location of the carbonate factory; however, as a whole, the platform continues to aggrade as the volcanic platform subsides with the plate. At this point, sea level can either rise or fall. If sea level rises and the carbonate factory cannot keep pace, then the carbonate factory backsteps in manner similar to the initial transgressive event. If sea level falls, subaerial exposure of the carbonate platform occurs and a karst surface forms. This surface marks the next major sequence boundary. In this case, the carbonate factory moves seaward of the slope break marking the edge of the summit plateau, and local carbonate production occurs on the guyot flank. These sediments are primarily transported to the basin as turbidites, although the sediment supply to the basin decreases as the area over which the carbonate factory operates is at a minimum (in contrast to silicic-dominated margins where sea-level lows result in high depositional rates for the basin). Consequently, a well-defined LST systems tract of slope fans and a prograding slope wedge is absent because the flanks of the volcano are sufficiently steep to bypass sediment directly to the adjacent deep ocean basin. Local cementation of the karstic caves (speleothems) and breccia lying on the karst surface might be representative of LST sediments on the platforms.

During a subsequent rise in sea level, the carbonate factory initially establishes itself along the perimeter of the existing carbonate platform. If the rate of sea-level rise surpasses the rate of carbonate production, the carbonate factory once again backsteps toward the center of the plateau. Assuming the basement high is still above sea level, the stratal pattern visible in the seismic data is similar to the initial flooding of the volcanic platform, except that the existing, eroded carbonate platform provides a flatter surface than the original volcanic platform.

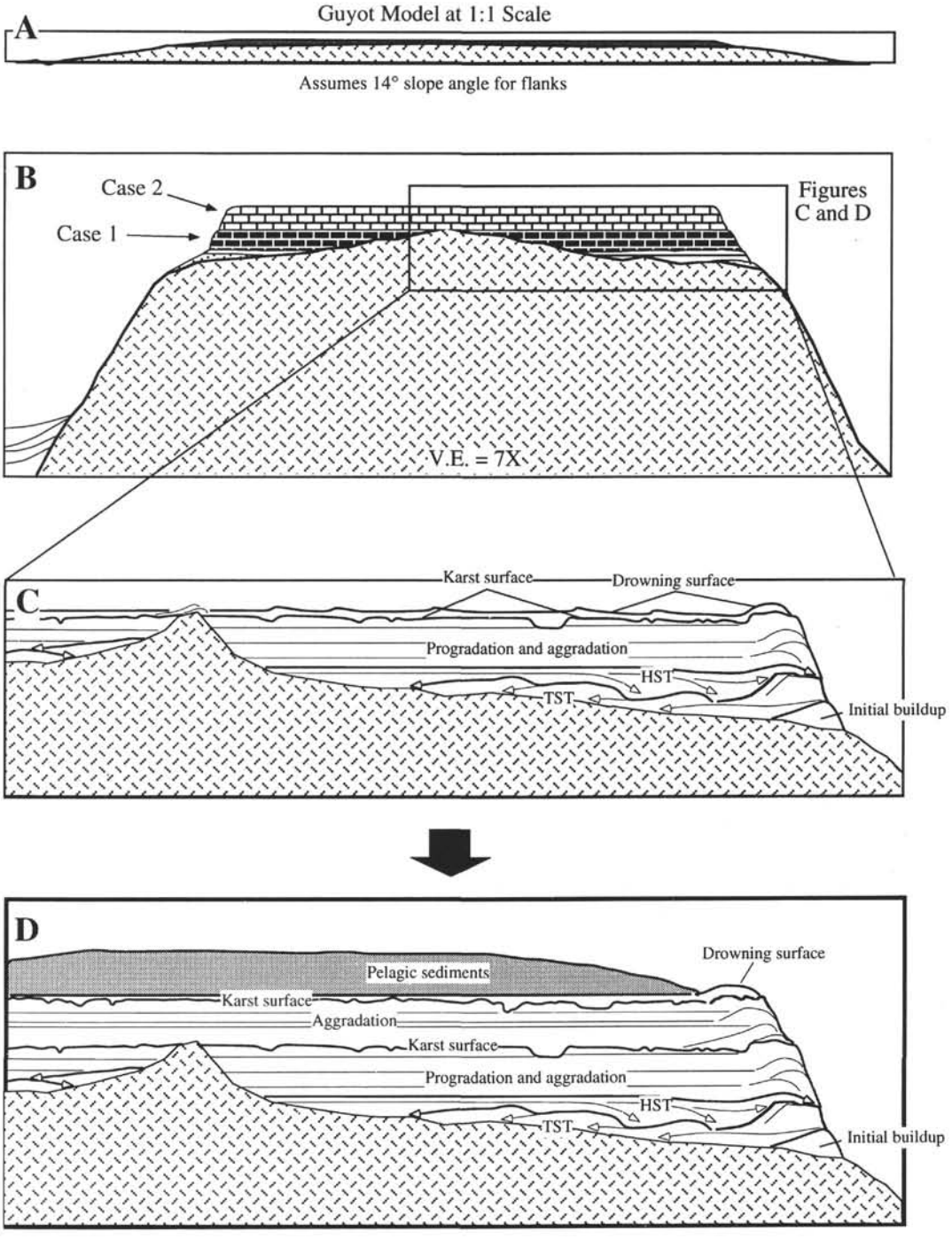

Figure 14. Small, mid-ocean carbonate platform model based on Wodejebato Guyot.

Consequently, the stacked shoal units appear only near the center of the summit plateau. If the basement high is submerged below sea level (and presumably covered by sediments), the dominant stratal patterns of the TST and HST systems tracts change from retrogradational and progradational to primarily aggradational (Fig. 14D). As noted previously, the failure of the platforms results from rates of sea-level rise outpacing carbonate accumulation rates. Because the carbonate factory cannot backstep onto a central basement high, the carbonate platform is more susceptible to failure at this point.

REFERENCES*

Arnaud Vanneau, A., and Arnaud, H., 1990. Hauterivian to Lower Aptian carbonate shelf sedimentation and sequence stratigraphy in the Jura and northern Subalpine chains (southeastern France and Swiss Jura). *In* Tucker,

* Abbreviations for names of organizations and publications in ODP reference lists follow the style given in *Chemical Abstracts Service Source Index* (published by American Chemical Society).

M.E., Wilson, J.L., Crevello, P.D., Sarg, J.R., and Read, J.F. (Eds.), *Carbonate Platforms: Facies, Sequences and Evolution.* Spec. Publ. Int. Assoc. Sedimentol., 9:203–233.

Arnaud Vanneau, A., and Carrio-Schaffauser, E., 1994. Reservoir aspects in relationship with sequence boundaries in carbonate platforms. *In* Mascle, A. (Ed.), *Hydrocarbon and Petroleum Geology of France.* Spec. Publ.—Euro. Assoc. Pet. Geosci., 4:321–323.

Bergersen, D.D., 1993. Geology and geomorphology of Wodejebato (Sylvania) Guyot, Marshall Islands. *In* Pringle, M.S., Sager, W.W., Sliter, W.V., and Stein, S. (Eds.), *The Mesozoic Pacific: Geology, Tectonics, and Volcanism.* Geophys. Monogr., Am. Geophys. Union. 77:367–385.

Bergersen, D.D., Larson, R.L., and Shipboard Scientific Party, 1992. Seismic stratigraphy of guyots drilled during ODP Leg 144: preliminary results. *Eos,* 73:587.

Durlet, C., Loreau, J.-P., and Pascal, A., 1992. Signature diagénétique des discontinuités et nouvelle représentation graphique de la diagénèse. *C. R. Acad. Sci. Ser. 2,* 314:1507–1514.

Hanford, C.R., and Loucks, R.G., 1993. Carbonate depositional sequences and systems tracts: responses of carbonate platform to relative sea-level changes. *In* Sarg, J.F., and Loucks, R.G. (Eds.), *Carbonate Sequence Stratigraphy.* AAPG Mem., 57:3–41.

Haq, B.U., Hardenbol, J., and Vail, P.R., 1987. The new chronostratigraphic basis of Cenozoic and Mesozoic sea level cycles. *Spec. Publ. Cushman Found. Foraminiferal Res.,* 24:7–13.

Jacquin, T., Arnaud Vanneau, A., Arnaud, H., Ravenne, C., and Vail, P.R., 1991. Systems tracts and depositional sequences in carbonate setting: a study of continuous outcrops from platform to basin at the scale of seismic lines. *Mar. Pet. Geol.,* 8:122–140.

Jacquin, T., and Vail, P.R., in press. Shelfal accommodation as a major control of carbonate platforms. *Bull. Soc. Geol. Fr.*

James, N.P., and Macintyre, I.G., 1985. Reefs: carbonate depositional environments, modern and ancient (Pt. 1). *Color. Sch. Mines Quart.,* 80.

Lincoln, J.M., Pringle, M.S., and Premoli-Silva, I., 1993. Early and Late Cretaceous volcanism and reef-building in the Marshall Islands. *In* Pringle, M.S., Sager, W.W., Sliter, W.V., and Stein, S. (Eds.), *The Mesozoic Pacific: Geology, Tectonics, and Volcanism.* Geophys. Monogr., Am. Geophys. Union, 77:279–305.

Nakanishi, M., and Gee, J.S., 1992. Paleolatitude of Guyots in the northwestern Pacific Ocean : preliminary results of ODP Leg 144. *Seismolog. Soc. Jpn.* (Abstract)

Okada, H., and Bukry, D., 1980. Supplementary modification and introduction of code numbers to the low-latitude coccolith biostratigraphic zonation (Bukry, 1973; 1975). *Mar. Micropaleontol.,* 5:321–325.

Premoli Silva, I., Haggerty, J., Rack, F., et al., 1993. *Proc. ODP, Init. Repts.,* 144: College Station, TX (Ocean Drilling Program).

Read, J.F., 1985. Carbonate platform facies models. *AAPG Bull.,* 69:1–21.

Sarg, J.F., 1988. Carbonate sequence stratigraphy. *In* Wilgus, C.K., Hastings, B.S., Kendall, C.G.St.C., Posamentier, H.W., Ross, C.A., and Van Wagoner, J.C. (Eds.), *Sea Level Changes: An Integrated Approach.* Spec. Publ.—Soc. Econ. Paleontol. Mineral., 42:155–181.

Shipboard Scientific Party, 1993. Site 869. *In* Sager, W.W., Winterer, E.L., Firth, J.V., et al., *Proc. ODP, Init. Repts.,* 143: College Station, TX (Ocean Drilling Program), 297–374.

Vail, P.R., Mitchum, R.M., Jr., and Thompson, S., III, 1977. Seismic stratigraphy and global changes of sea level. Part 3: Relative changes of sea level from coastal onlap. *In* Payton, C.E. (Ed.), *Seismic Stratigraphy—Applications to Hydrocarbon Exploration.* AAPG Mem., 26:63–81.

Van Wagoner, J.C., Posamentier, H.W., Mitchum, R.M., Jr., Vail, P.R., Sarg, J.F., Loutit, T.S., and Hardenbol, J., 1988. An overview of the fundamentals of sequence stratigraphy and key definitions. *In* Wilgus, C.K., Hastings, B.S., Ross, C.A., Posamentier, H.W., Van Wagoner, J., and Kendall, C.G.St.C. (Eds.), *Sea-Level Changes: An Integrated Approach.* Spec. Publ.—Soc. Econ. Paleontol. Mineral., 42:39–45.

Vollbrecht, R., and Meischner, D., 1993. Sea level and diagenesis: a case study on Pleistocene beaches, Whalebone Bay, Bermuda. *Geol. Rundsch.,* 82:248–262.

Walker, R.G., 1990. Facies modeling and sequence stratigraphy. *J. Petrol.,* 60:777–786.

Wilgus, C.K., Posamentier, H., Ross, C.A., and Kendall, C.G.St.C. (Eds.), 1988. *Sea Level Changes: An Integrated Approach.* Spec. Publ.—Soc. Econ. Paleontol. Min., 42.

Date of initial receipt: 3 August 1994
Date of acceptance: 2 January 1995
Ms 144SR-001

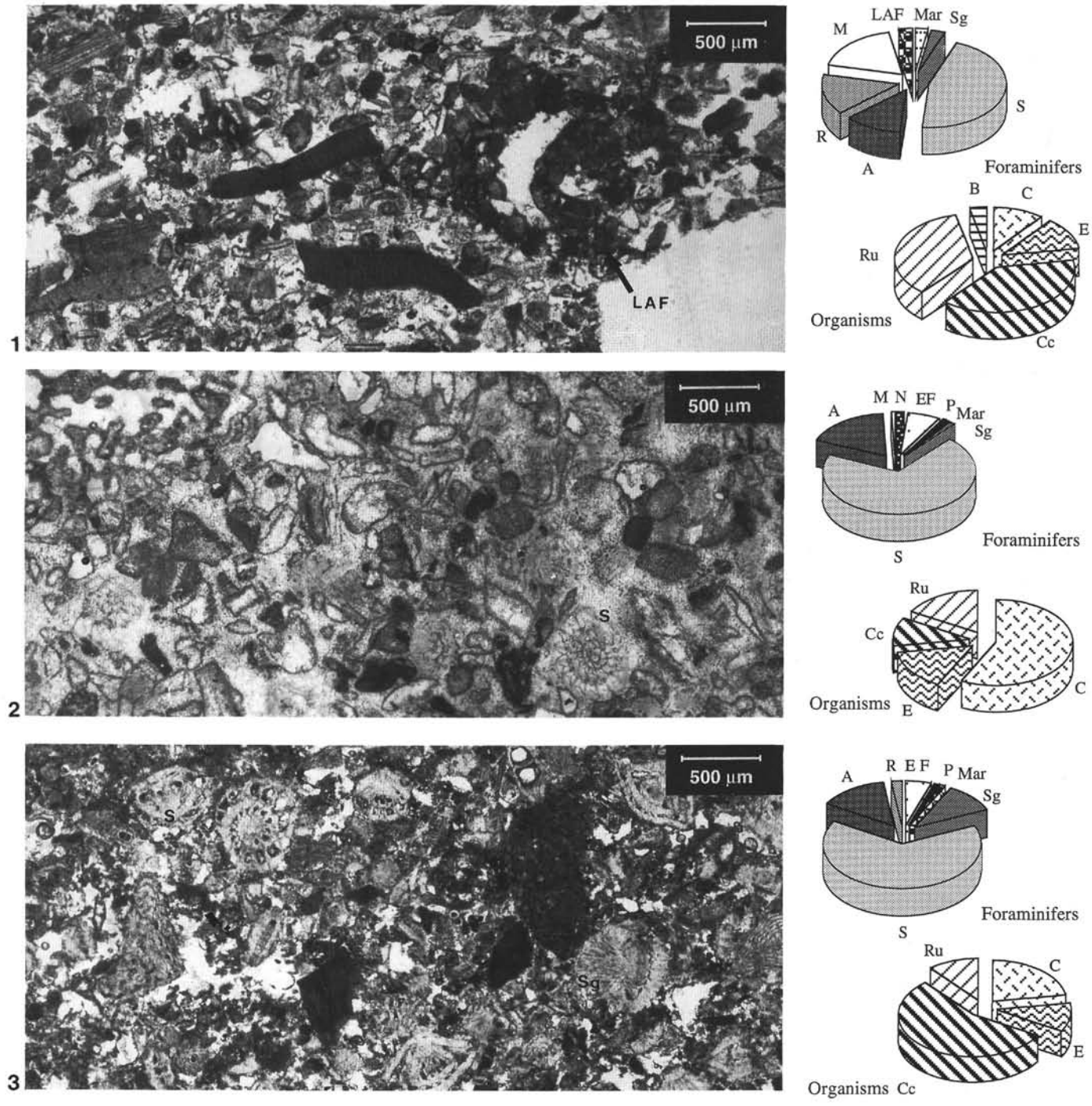

Plate 1. Distribution of organisms in the carbonate facies of Wodejebato (Hole 874B). **1.** Sample 144-874B-17R-1, 24–27 cm (top of LST or bottom of TST systems tract), grainstone with rudist, corallinacean algae, and echinoid fragments. **2.** Sample 144-874B-7R-1, 26–31 cm (TST systems tract), grainstone with rudist, corallinacean algae, and coral fragments. **3.** Sample 144-874B-9R-1, 99–101 cm (TST systems tract), packstone with *Asterorbis* and *Sulcoperculina.* A = *Asterorbis,* B = bivalves, C = coral, Cc = corallinacean algae, D = dasycladacean algae, E = echinoids, EF = encrusting foraminifers, LAF = large agglutinated foraminifers, M = miliolids, Mar = *Marssonella,* N = nodosariids, P = planktonic foraminifers, R = rotaliids, Ru = rudists, S = *Sulcoperculina,* and Sg = *S. globosa.*

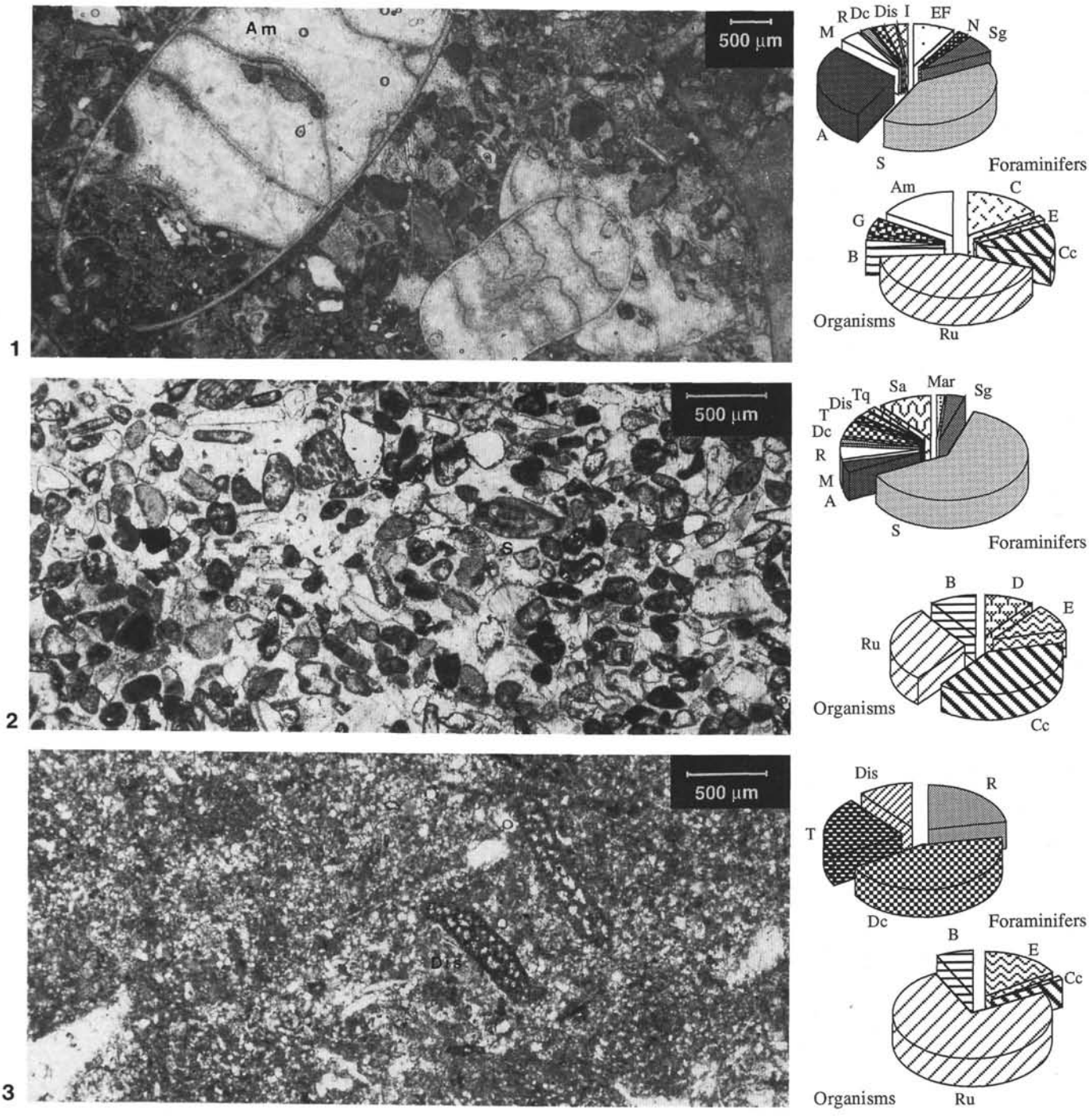

Plate 2. Distribution of organisms in the carbonate facies of Wodejebato (Holes 873A and 874B). **1.** Sample 144-874B-6R-2, 1–3 cm (maximum flooding surface), packstone with ammonites. **2.** Sample 144-873A-10R-1, 10–12 cm (TST systems tract), grainstone with rare *Sulcoperculina.* **3.** Sample 144-873A-9R-2, 67–71 cm (TST systems tract), wackestone with *Dicyclina.* A = *Asterorbis,* Am = ammonites, B = bivalves, C = coral, Cc = corallinacean algae, Dc = *Dicyclina,* Dis = discorbids, E = echinoids, EF = encrusting foraminifers, G = gastropods, I = *Istriloculina,* M = miliolids, Mar = *Marssonella,* N = nodosariids, R = rotaliids, Ru = rudists, S = *Sulcoperculina,* Sa = *Salpingoporella,* Sg = *S. globosa,* T = textulariids, and Tq = *Terquemella.*

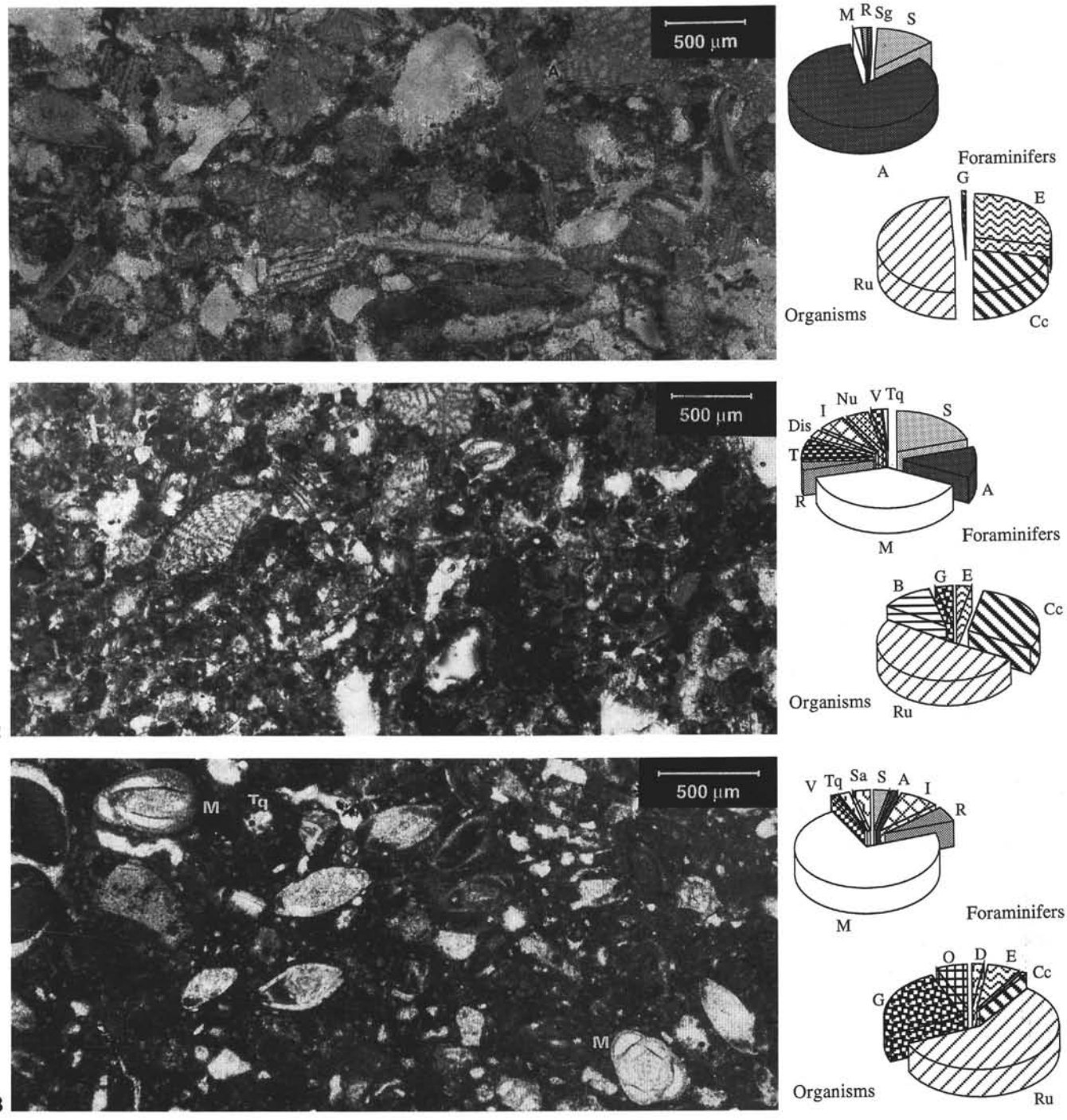

Plate 3. Distribution of organisms in the carbonate facies of Wodejebato (Holes 873A and 874B). **1.** Sample 144-873A-9R-2, 0–3 cm (TST systems tract), packstone-wackestone with dasycladacean algae. **2.** Sample 144-874B-6R-1, 16–19 cm (probable early HST systems tract), grainstone with rudists and *Asterorbis*. **3.** Sample 144-874B-6R-1, 47–52 cm (probable early HST systems tract), grainstone with rudist fragments, *Asterorbis,* and *Sulcoperculina.* A = *Asterorbis,* B = bivalves, C = coral, Cc = corallinacean algae, D = dasycladaceans, E = echinoids, G = gastropods, I = *Istriloculina,* M = miliolids, R = rotaliids, Ru = rudists, S = *Sulcoperculina,* Sa = *Salpingoporella,* Sg = *S. globosa,* T = textulariids, and Tq = *Terquemella.*

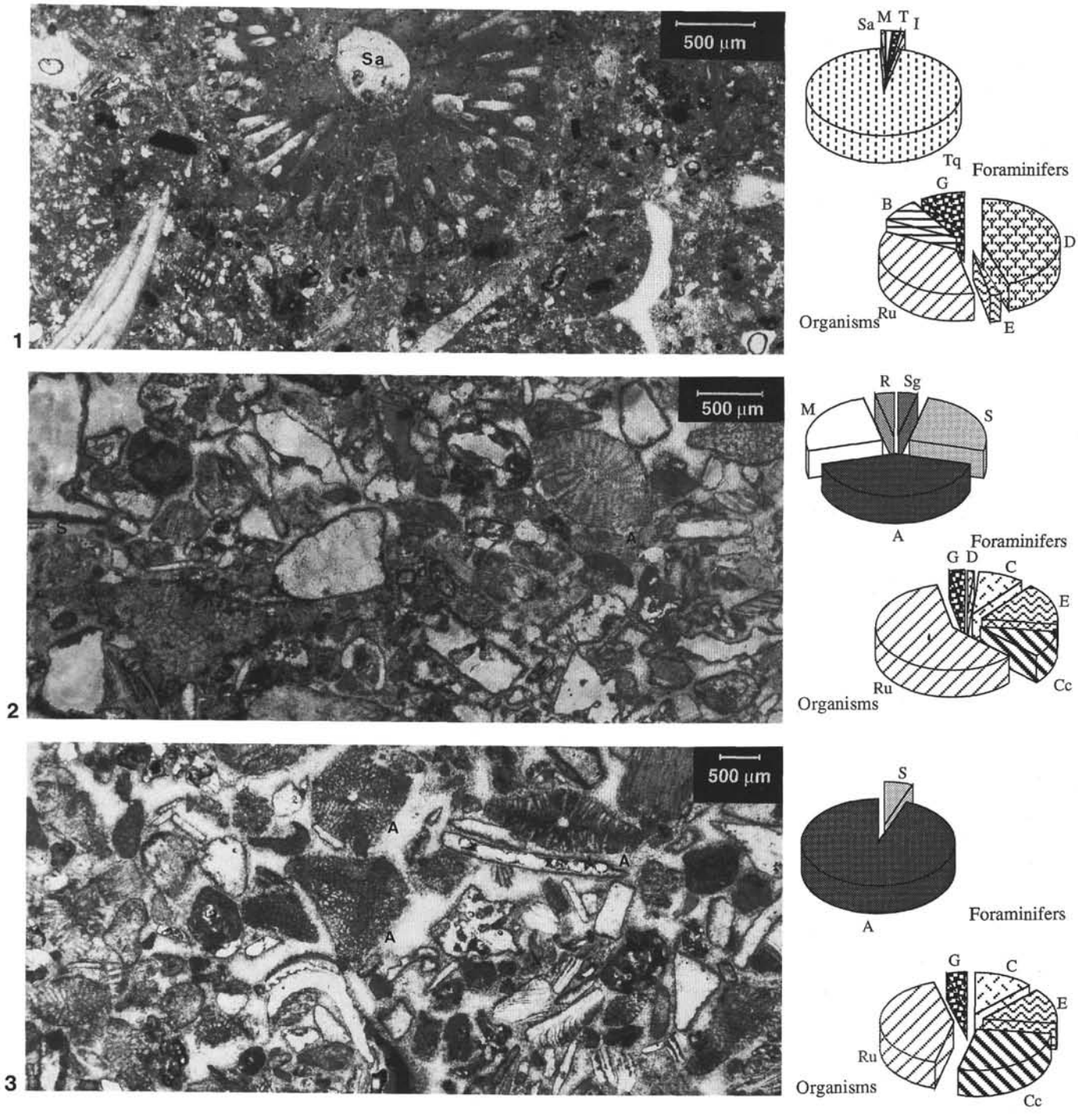

Plate 4. Distribution of organisms in the carbonate facies of Wodejebato (Holes 873A and 874B). **1.** Sample 144-874B-3R-3, 19–22 cm (late HST systems tract), packstone with rudists, *Sulcoperculina,* and *Asterorbis.* **2.** Sample 144-873A-5R-1, 78–82 cm (late HST systems tract), grainstone with rudist fragments, *Sulcoperculina, Asterorbis,* and miliolids. **3.** Sample 144-873A-6R-1, 103–106 cm (HST systems tract), wackestone with miliolids. A = *Asterorbis,* B = bivalves, Cc = corallinacean algae, D = dasycladacean algae, Dis = discorbids, E = echinoids, G = gastropods, I = *Istriloculina,* M = miliolids, Nu = *Nummoloculina,* O = ostracods, R = rotaliids, Ru = rudists, S = *Sulcoperculina,* Sa = *Salpingoporella,* Sg = *S. globosa,* T = textulariids, Tq = *Terquemella,* and V = *Vidalina.*

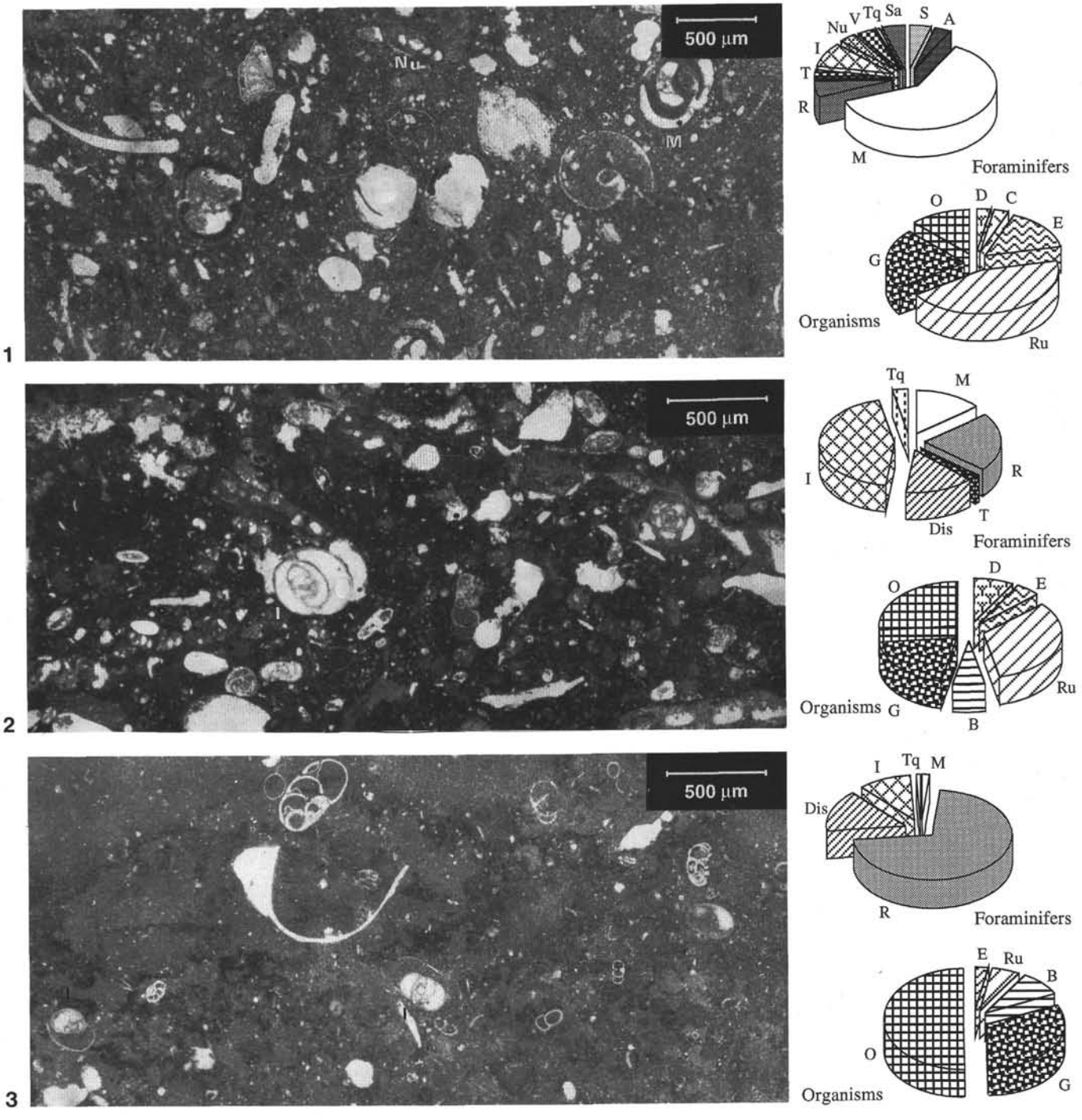

Plate 5. Distribution of organisms in the carbonate facies of Wodejebato (Hole 874B). **1.** Sample 144-874B-4R-1, 23–31 cm (early HST systems tract), wackestone with miliolids, *Sulcoperculina,* and gastropods. **2.** Sample 144-874B-2R-2, 47–55 cm (early HST systems tract), wackestone with miliolids, rotaliids, and discorbids. **3.** Sample 144-874B-3R-3, 19–22 cm, mudstone-wackestone with gastropods, rotaliids, discorbids, and *Istriloculina.* B = bivalves, C = coral, D = dasycladaceans, Dis = discorbids, E = echinoids, G = gastropods, I = *Istriloculina,* M = miliolids, Nu = *Nummoloculina,* O = ostracodes, R = rotaliids, Ru = rudists, T = textulariids, Tq = *Terquemella,* and V = *Vidalina.*